Lévy Processes and Quantum Mechanics: An Investigation Into the Distribution of Log Returns

Christiaan Hugo le Roux

Thesis presented in the partial fulfilment
of the requirement for the degree of
MCom (Financial Risk Management)
at the University of Stellenbosch

Supervisor : Prof. T. De Wet

Degree of confidentiality: A

March 2021

PLAGIARISM DECLARATION

1. Plagiarism is the use of ideas, material and other intellectual property of another's work and to present it as my own.
2. I agree that plagiarism is a punishable offence because it constitutes theft.
3. Accordingly, all quotations and contributions from any source whatsoever (including the internet) have been cited fully. I understand that the reproduction of text without quotation marks (even when the source is cited) is plagiarism.
4. I also understand that direct translations are plagiarism.
5. I declare that the work contained in this thesis, except otherwise stated, is my original work and that I have not previously (in its entirety or in part) submitted it for grading in this thesis or another thesis.

C.H. le Roux	3 November 2020
Initials and surname	Date

ACKNOWLEDGEMENTS

I would like to thank Professor T. De Wet for taking the time out of his busy schedule to supervise and provide guidance for this research project.

I would also like to thank my family for providing the moral and financial support needed to complete this project.

I would like to thank Daniel de Kock and Johann Bierman for assisting with proof reading.

Finally, I would like to thank the reddit communities; *r/askmath* and *r/askscience* who helped me understand many of the complex mathematical concepts underlying Quantum Mechanics and Lévy Processes.

The Department of Statistics and Actuarial Science (the Department) wishes to acknowledge David Rodwell for generously creating a template based off the USB (University of Stellenbosch Business School) guidelines which have been adapted for the purposes of the department.

ABSTRACT

It is well known that log returns on stocks do not follow a normal distribution as is assumed under the Black-Scholes pricing formula. This study investigates alternatives to Brownian Motion which are better suited to capture the stylized facts of asset returns. Lévy processes and models based on Quantum Mechanical theory are described and fit to daily log returns for various JSE Indices. Maximum likelihood estimation is used to estimate the parameters of the Lévy processes and the Cramer-von Mises goodness of fit statistic is minimized to estimate the parameters of the Quantum Mechanical models. Q-Q plots and the Kolmogorov-Smirnov fit statistic is presented to assess the fit of the various models. The results show that the Lévy processes, specifically the Normal Inverse Gaussian process, are the best among the processes considered. The performance of the Quantum Mechanical models could be improved if more eigenstates are considered in the approximation, however the computational expense of these models makes them impractical.

Key words:

Log Return Distribution; Lévy Processes; Stock Indices; Quantum Finance

OPSOMMING

Dit is bekend dat log opbrengste op aandele nie 'n normale verdeling volg soos in die Black-Scholes prysingsformule aanvaar word nie. Hierdie studie ondersoek alternatiewe tot Brownse Beweging wat beter geskik is om die gestileerde feite van bate opbrengste vas te lê. Lévy prosesse en modelle gebaseer op die kwantummeganiese teorie word beskryf en aangepas tot daaglikse log opbrengste vir verskillende JSE-indekse. Maksimale aanneemlikheid beraming word gebruik om die parameters van die Lévy-prosesse te beraam, en die Cramer-von Mises passingstoets grootheid word geminimeer om die parameters van die kwantummeganiese modelle te beraam. Q-Q stippings en Kolmogorov-Smirnov passingsstatistieke word gebruik om die pasgehalte van die verskillende modelle te evalueer. Die resultate toon dat die Lévy prosesse, spesifiek die Normaal Inverse Gaussiese proses, die beste presteer onder die prosesse wat oorweeg word. Die kwantummeganiese modelle kan beter presteer as meer eie state in die benadering gebruik word, maar die berekeningskoste van hierdie modelle maak dit onprakties.

Sleutelwoorde:
Log Opbrengs Verspreiding; Lévy Prosesse; Aandeelindekse; Kwantumfinansiering

TABLE OF CONTENTS

LIST OF FIGURES

LIST OF TABLES

LIST OF APPENDICES

LIST OF ABBREVIATIONS AND/OR ACRONYMS

API	Application Programming Interface
CGMY	Carr Gaman Madan Yor
FTSE	Financial Times Stock Exchange
GH	Generalized Hyperbolic
GIG	Generalized Inverse Gaussian
i.i.d	Independent and Indentically Distributed
IG	Inverse Gaussian
JSE	Johannesburg Stock Exchange
KE	Kinetic Energy
KS	Kolmogorov-Smirnov
MLE	Maximum Likelihood Estimate (Estimation)
NIG	Normal Inverse Gaussian
pdf	Probability Density Function
PE	Potential Energy
QAHO	Quantum An-Harmonic Oscillator
QHO	Quantum Harmonic Oscillator
SWIX	Shareholder Weighted Index
VG	Variance Gamma
GPD	General Pareto Distribution

CHAPTER 1

INTRODUCTION

This assignment aims to investigate alternatives to the Brownian Motion process underlying the Black Scholes option pricing formula. It is well known that log returns on stocks and stock indices are not normally distributed as is assumed under the Black Scholes framework [Cont (2001)]. This assignment considers two broad groups of models describing the log return process on South African indices; Lévy processes and models based on quantum mechanical theory. The interest is in finding a model which describes the distribution well over the entire range of the log return data.

The assignment is structured as follows: The remainder of Chapter 1 discusses the stylized facts of asset returns. Following that, Chapter 2 introduces Lévy processes. These are a subset of Stochastic processes that adequately capture some of the stylized facts of asset returns. Chapter 3 introduces applications of quantum mechanics to modelling asset returns. Chapter 4 presents the goodness of fit of the selected models once applied to popular South African stock indices. The indices used in the study are: JSE Top 40, JSE Shareholder Weighted Index (SWIX), JSE Banks, JSE Financials, JSE Indutrials and JSE Resources. Q-Q plots and the Kolmogorov Smirnov (KS) goodness of fit statistic are the primary measures used to assess goodness of fit. Chapter 5 concludes the paper.

1.1 STYLIZED FACTS

Certain statistical properties have been observed in empirical studies conducted on the log returns of stocks. These properties are commonly referred to as the stylized facts of asset returns. This section outlines some of these facts as they pertain to the JSE Top 40 Index over the period 01 January 2010 to 01 June 2020. For a detailed discussion on the stylized facts of asset returns, the reader is referred to Cont (2001).

From Figure 1.1 it is clear that daily log returns are not normally distributed. The coefficient of skewness is -0.5346, but the skewness is not obvious from the plot. The excess kurtosis is 6.7937 and it is clear from the plot that the data is leptokurtic. Another crucial assumption underlying the Black-Scholes formula is that the volatility of a particular asset is constant [Hull (2009)]. Figure

1.2 shows that volatility is in fact not constant and that spikes in volatility occur in clusters.

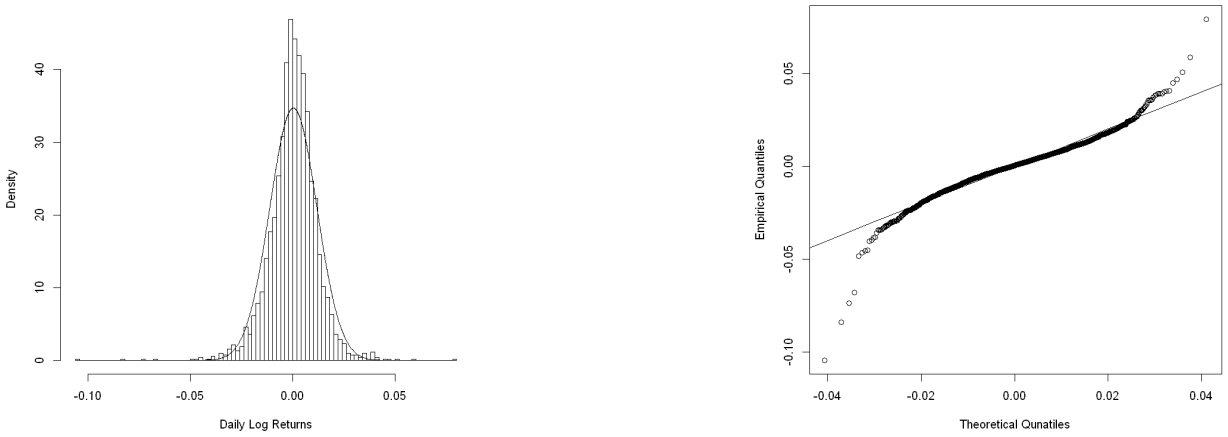

(a) Density Plot

(b) Q-Q Plot

Figure 1.1: Normal distribution fit to the JSE Top 40 daily log returns. $\hat{\mu} = 0.0239\%$ and $\hat{\sigma} = 1.1494\%$.

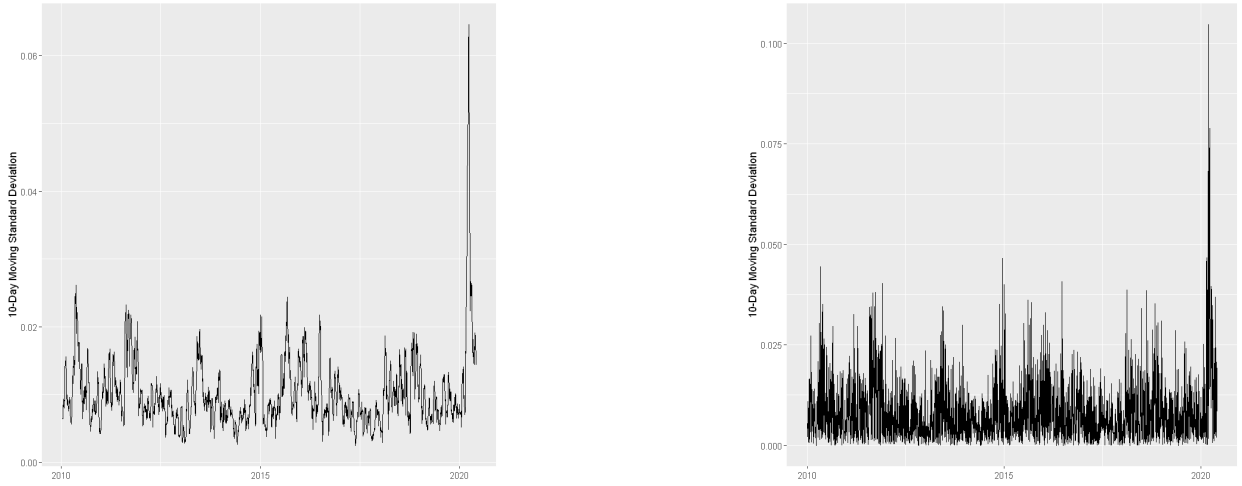

(a) 10 day moving standard deviation of JSE Top 40 daily log returns.

(b) $(r-\hat{\mu})^2$, with r the daily log return on the JSE Top 40 index.

Figure 1.2: Stochastic volatility on the daily log returns of the JSE Top 40 index.

This section presents evidence that Brownian Motion is not an appropriate description for the log return process of the JSE Top 40 Index. The Stylized Facts of Asset Returns are present in most stocks and stock indices [Cont (2001)]. Chapter 2 introduces alternative stochastic processes which attempt to describe the process of the log stock price, form which the distribution of the daily log returns can easily be obtained.

CHAPTER 2

LÉVY PROCESSES

Lévy processes are a subset of stochastic processes that have useful properties which capture some of the stylized facts of asset returns outlined in Chapter 1.

The first section introduces the general theory behind Lévy processes. Some examples of Lévy processes are provided in the subsequent sections.

The models outlined below attempt to model the stochastic dynamics of L_t, where:

$$L_t = \log(S_t) \tag{2.1}$$

with S_t the price of the index at the close of day t. The daily log return at time t refers to $L_t^* = L_{t+1} - L_t$, which has the same distributions as L_1.[1] It is the distribution of the daily log return that is the primary focus of this study.

2.1 LÉVY PROCESSES

Consider a stochastic process $L = (L_t)_{t\epsilon\mathbb{R}_+}$ with state space $\left(\mathbb{R}^d, \mathcal{B}\right)$. $\mathcal{B}$ is the Borel σ-algebra and L is adapted to the filtration $\mathcal{F} = (\mathcal{F}_t)_{t\epsilon\mathbb{R}_+}$. Çinlar (2011) defines L to be a Lévy process with respect to $\mathcal{F}$ if it has the following properties:

- The sample paths are left-limited and right continuous.
- $L_{t+u} - L_t$ is independent of $\mathcal{F}_t$ and has the same distribution as L_u for all t and u in $\mathbb{R}_+$.[2]

A stochastic process that satisfies the first point is referred to as a pure jump processes. The second point states that the process has independent increments and is stationary. Well known examples of Lévy processes include the Poisson Process, the Compound Poisson Process and Brownian Motion.

[1] It is useful to note that L_0 is assumed to be zero [Çinlar (2011)].
[2] This allows L_t^* to be modelled using the same distribution as L_1.

2.1.1 Characteristic Equation and the Lévy-Khintchine Theorem

A random variable is said to be infinitely divisible if it can be written as a sum of n i.i.d random variables, for every $n \epsilon \mathbb{N}$. Recall that the increments of a Lévy process are independent and the Lévy process is stationary. Thus, L_t can always be expressed as a sum of i.i.d random variables and is infinitely divisible. It follows that L_t has a characteristic function of the form [Çinlar (2011)]:

$$\phi(r) = \mathbb{E}\left[e^{irL_t}\right] = e^{t\psi(r)}; \quad t \epsilon \mathbb{R}_+, \ r \epsilon \mathbb{R} \tag{2.2}$$

$\psi(r)$ is called the characteristic exponent of the Lévy process. The Lévy-Khintchine formula states that the characteristic exponent from Equation (2.2) takes the form [Çinlar (2011)]:

$$\psi(r) = ir\mu - \frac{1}{2}r^2\sigma + \int_{|x|\leq 1}\left(e^{irx} - 1 - irx\right)\nu(dx) + \int_{|x|>1}\left(e^{irx} - 1\right)\nu(dx), \quad r \epsilon \mathbb{R} \tag{2.3}$$

where ν is the Lévy measure with corresponding Lévy density $\pi(x)$ i.e. $\pi(x)dx = \nu(dx)$. Equation (2.3) shows that a Lévy process is fully determined by the mathematical triple (μ, σ, ν). The terms in the mathematical triple determine the drift, volatility[3] and jumps respectively. Equation (2.2) shows that once $\psi(r)$ is defined, the densities of L_t can be found for any $t > 0$ by taking the Inverse Fourier Transform of $\phi(r)$.

2.1.2 Finite Activity, Finite Variation and Finite Quadratic Variation

A Lévy process is said to exhibit finite activity when the integral of the Lévy density is finite [Wu (2007)]:

$$\int_{\mathbb{R}_0} \pi(x)dx = \lambda < \infty \tag{2.4}$$

where λ is the mean arrival rate rate of jumps and $\mathbb{R}_0 = \mathbb{R} \setminus 0$. Finite activity means that over any finite time period, a finite number of jumps will be observed. When the integral in Equation (2.4) is infinite, the process is said to exhibit infinite activity, and generates an infinite number of jumps over any finite period of time.

[3] σ is often referred to as the diffusion term in academic literature.

The process is said to exhibit finite variation if the following inequality holds [Wu (2007)]:

$$\int_{\mathbb{B}} x\pi(x)dx < \infty. \tag{2.5}$$

When a process exhibits infinite variation, the sum of jumps does not converge. The sum of jumps with their respective means subtracted does converge, however.

In order for the Lévy process to be a semimartingale, the following condition must be met [Wu (2007)]:

$$\int_{\mathbb{R}_0} x^2\pi(x)\mathbb{I}_{x^2\leq 1}dx < \infty \tag{2.6}$$

when Equation (2.6) is met, the process is said to exhibit finite quadratic variation.

2.1.3 Stochastic Time Change

As is discussed in Section 2.1.1, a Lévy process is fully determined by the mathematical triplet (μ, σ, ν). The parameters μ and σ are both constant values, however Chapter 1 showed that the variance of financial assets is not constant.

One approach to building stochastic volatility into a L'evy process is to make use of stochastic time change. Consider two independent Lévy processes, X_t and T_t where T_t is a monotonically increasing process. We can define a new process Y_t to be the process X_t evaluated at time T_t [Wu (2007)]:

$$Y_t = X_{T_t}. \tag{2.7}$$

The process T_t is called the subordinator and determines the time at which X_t is evaluated. This allows for the incorporation of stochastic volatility.

2.2 BROWNIAN MOTION

Brownian Motion[4] is a stochastic process in discrete time with the following two properties [Hull (2009)]:

- $\Delta z = \epsilon\sqrt{\Delta t}$, where $\epsilon \sim N(0,1)$.
- The values of Δz are independent over small non-intersecting periods of time, Δt.

Drift and volatility terms can be added to give the following differential equation for the price of a stock in continuous time [Hull (2009)]:

$$dS_t = \mu S_t dt + \sigma S_t dz \tag{2.8}$$

where S_t is the price of the stock at time t, dz is continuous time Brownian Motion, μ is the drift rate[5] and σ is the volatility. σ^2 is referred to as the variance rate. The variance rate gives an indication to the amount of price movement, and thus indicates the level of market risk.

Itô's lemma is used to find the process for $L_t = \ln S_t$ [Hull (2009)]:

$$dL_t = \left(\mu - \frac{\sigma^2}{2}\right) dt + \sigma dz \tag{2.9}$$

or

$$L_t = \mu^* t + \sigma B_t \tag{2.10}$$

where B_t is Brownian Motion and $\mu^* = \mu - \frac{\sigma^2}{2}$.

Equation (2.9) implies that the log return between time $t = 0$ and $t = T$ has a Normal distribution [Hull (2009)]:

$$\ln S_T - \ln S_0 \sim N\left[\left(\mu - \frac{\sigma^2}{2}\right) T, \sigma^2 T\right] \tag{2.11}$$

[4]Brownian motion is also sometimes referred to as a Wiener Process.
[5]μ is the expected continuously compounded rate of return.

which implies that the distribution of S_T is log-normal.

Brownian Motion provides a useful starting point for modelling the distribution of log returns, but it is well known that the log returns of stock prices are in fact not normally distributed. Recall from Chapter 1 that in reality skewness and excess kurtosis are typically observed. Furthermore, recall from Figure (**??**) that volatility is not constant.[6] Brownian Motion is therefore not an appropriate representation of stock price log returns.

2.3 MERTON'S MODEL

Merton (1976) proposed the use of Brownian Motion coupled with a Compound Poisson Process to model stock prices. This model is provided as a brief introduction to the notion of jump processes.

Compound Poisson Process: Consider $N_t \sim \text{Poisson}(\lambda t)$, where N_t denotes the number of jumps in the time interval $(0, t]$. Furthermore consider $X_1, X_2, ...$; which are all i.i.d. random variables. A Compound Poisson Process Y_t is defined as follows [Pinsky and Karlin (2010)]:

$$Y_t = \sum_{n=1}^{N_t} X_n. \tag{2.12}$$

Coupling Equation (2.12) to the Brownian Motion model adds N_t jumps in the time period $(0, t]$. The log stock price at time point t will then be the value taken on by the Brownian Motion at time t plus the cumulative sum of jumps up to time t, i.e. Y_t in Equation (2.12).

The process for the log stock price L_t is therefore:

$$L_t = \mu t + \sigma B_t + \sum_{i=0}^{N_t} J_i \tag{2.13}$$

where B_t is Brownian Motion as discussed in Section 2.2, N_t is a Poisson Process as in Equation (2.12) and J_i is some sequence of i.i.d random variables. In this case, $J_i \sim N(\mu_J, \sigma_J)$ where μ_J is

[6] Refer to Engle (2004) for a more in depth discussion of stochastic volatility.

the mean jump size and σ_J is the standard deviation of jumps. A fifth parameter, λ, denotes the arrival rate in the Poisson Process N_t.

It can be shown that the Lévy density and characteristic exponent for the jump component can be written as follows [Wu (2007)]:

$$\pi(x) = \lambda \frac{1}{\sqrt{2\pi\sigma_J^2}} \exp\left(-\frac{(x-\mu_J)^2}{2\sigma_J^2}\right), \tag{2.14}$$

$$\psi(r) = \lambda\left(1 - e^{ir\mu_J - \frac{1}{2}r^2 v_J}\right). \tag{2.15}$$

The Poisson jump process described above exhibits finite activity, meaning it generates finite jumps over a finite period of time [Wu (2007)].

This model gives a better representation of the movement of stock prices than Brownian Motion since it allows for events such as corporate defaults where there is a large change in the stock price over a short time period. However, other than observing large jumps when significant events occur, in practice one would observe many small jumps over small periods of time. This is due to the fact that the stock price is renegotiated and will jump by a small amount each time it is traded.

The addition of the compound Poisson process allows for rare, significant events that cause a sudden, large, change in the asset price - e.g. corporate defaults or market crashes. The frequency of the jumps are determined by the parameter λ and the size of the jumps are determined by the specified distribution for jump sizes, in this case $N(\mu_J, \sigma_J)$ [Wu (2007)].

Wu (2007) provides a brief discussion on how small jumps due to trading require infinite variation to be exhibited by the selected model. Furthermore, stochastic variance must be built into a model for it to be an appropriate representation of movements in the stock market. There are alternative five parameter models that satisfy both of these properties, which is why Merton's Model is not investigated in Chapter 4.

2.4 CGMY (CARR, GEMAN, MADAN AND YOR) MODEL

The description of the CGMY model presented below is taken from Wu (2007). The Lévy density for the CGMY model is:

$$\pi(x) = \begin{cases} \lambda \exp(-\beta_+ x) x^{-\alpha-1}, & x > 0, \\ \lambda \exp(-\beta_- |x|) |x|^{-\alpha-1}, & x \leq 0 \end{cases}$$

with $\lambda, \beta_+, \beta_- > 0$ and $\alpha \, \epsilon \, [-1, 2]$. In this case, the parameter α controls the frequency of small jumps. When $\alpha \, \epsilon \, [0, 1)$, the stochastic process exhibits finite activity and finite variation. When $\alpha \, \epsilon \, [1, 2]$ the process exhibits infinite activity and infinite variation. Finite quadratic variation is imposed by ensuring $\alpha \leq 2$. The larger α, the more frequent the small jumps. The two exponential components (β_- and β_+) control the arrival rates of large jumps. Having separate β's for x positive or negative allows for the jump process to be skewed.

The above Lévy density is often referred to as a dampened power law Lévy density, and the characteristic exponent associated with it when $\alpha \neq 0$ and $\alpha \neq 1$ is:

$$\psi(r) = -\Gamma(-\alpha)\lambda \left[(\beta_+ - ir)^\alpha - \beta_+^\alpha + (\beta_- + ir)^\alpha - \beta_-^\alpha \right] - irC(h) \tag{2.16}$$

with $\Gamma(\alpha) \equiv \int_0^\infty x^{\alpha-1} e^{-x} dx$ the well known gamma function and a linear term $C(h)$, which is induced by some truncation function $h(x)$ for jumps with infinite-variation i.e. when $\alpha > 1$. The need for the truncation $h(x)$ is to ensure that the integral in Equation (2.5) is finite.[7]

A common choice for $h(x)$ is $h(x) = x\mathbb{I}_{\{|x|<1\}}$ so that:

$$C(h) = \lambda \left[\beta_+ (\Gamma(-\alpha)\alpha + \Gamma(1-\alpha, \beta_+)) - \beta_- (\Gamma(-\alpha)\alpha + \Gamma(1-\alpha, \beta_-)) \right], \quad \alpha > 1 \tag{2.17}$$

where $\Gamma(a, b) \equiv \int_b^\infty x^{\alpha-1} e^{-x} dx$ is the incomplete gamma function.

[7] This is to ensure that the jumps that occur an infinite amount of times over any finite amount of time does not cause the process to diverge.

When $\alpha = 0$, the characteristic exponent is:

$$\psi(r) = \lambda \ln(1 - ir/\beta_+)(1 + ir/\beta_-) = \lambda(\ln(\beta_+ - ir) - \ln \beta_+ + \ln(\beta_- + ir) - \ln \beta_-) \tag{2.18}$$

Since this process has finite variation, there is no need for the truncation.

When $\alpha = 1$, the characteristic exponent is:

$$\psi(r) = -\lambda((\beta_+ - ir) \ln(\beta_+ - ir)/\beta_+ + \lambda(\beta_- + ir) \ln(\beta_- + ir)/\beta_-) - irC(h) \tag{2.19}$$

where $C(h) = \lambda(\Gamma(0, \beta_+) - \Gamma(0, \beta_-))$ and the truncation function is $h(x) = x\mathbb{I}_{\{|x|<1\}}$.

The canonical form of the model is:

$$L_t = \theta Z(t) + \nu W(Z(t)) \tag{2.20}$$

The probability distribution and probability density are unknown for both the L_t and the subordinator T_t. A numerical estimate of the pdf can be obtained as in Ballotta and Kyriakou (2014) by specifying a grid for r in Equations (2.16), (2.18) or (2.19) - depending on the parameters - and computing the Inverse Fourier Transform. Due to the computational expense and loss of accuracy in the numerical approximations, the CGMY model is not considered as a competitor model to the other Lévy models presented above. The CGMY model is only presented to illustrate that once ψ in Equation (2.3) is specified, the Lévy process is fully defined.

2.4.1 Special Cases

The Variance Gamma process is a special case of the CGMY process where $\alpha = 0$ [Schoutens (2003)]:

$$VG(\lambda, \beta_+, \beta_-) \Longleftrightarrow CGMY(\lambda, \beta_+, \beta_-, 0). \tag{2.21}$$

The Variance Gamma process will be discussed in more detail later in Section 2.5.1.2.

2.5 GENERALIZED HYPERBOLIC PROCESS

The generalized hyperbolic density has the following form [Prause (1999)]:

$$\begin{aligned} f_{GH}(x;\lambda,\alpha,\beta,\delta,\mu) =& a\left(\lambda,\alpha,\beta,\delta\right)\left(\delta^2+(x-\mu)^2\right)^{\left(\lambda-\frac{1}{2}\right)/2} \\ & \times K_{\lambda-\frac{1}{2}}\left(\alpha\sqrt{\delta^2+(x-\mu)^2}\right)\exp\left(\beta(x-\mu)\right) \end{aligned} \tag{2.22}$$

with

$$a(\lambda,\alpha,\beta,\delta) = \frac{\left(\alpha^2-\beta^2\right)^{\lambda/2}}{\sqrt{2\pi}\alpha^{\lambda-1/2}\delta^{\lambda}K_{\lambda}\left(\delta\sqrt{\alpha^2-\beta^2}\right)}, \tag{2.23}$$

where K_λ is a modified Bessel function. The parameters have the following properties:

- $\mu \,\epsilon\, \mathbb{R}$
- $\delta \geq 0,\ |\beta| < \alpha$ if $\lambda > 0$
- $\delta > 0,\ |\beta| < \alpha$ if $\lambda = 0$
- $\delta > 0,\ |\beta| \leq \alpha$ if $\lambda < 0$

The Generalized Hyperbolic Density can be written as a normal mean-variance mixture, where the mixing density is Generalized Inverse Gaussian [Prause (1999)]:

$$f_{GH}(x;\lambda,\alpha,\beta,\delta,\mu) = \int_0^\infty f_{Norm}(x;\mu+\beta\omega,\omega) f_{GIG}(\omega;\lambda,\delta^2,\alpha^2-\beta^2)d\omega \tag{2.24}$$

When $\beta > 0$, the mean of the normal distribution $(\mu+\beta\omega)$ increases as ω increases and vice versa when $\beta < 0$. This, to an extent, describes the relationship between risk and return for the stock in question.

The Generalized Inverse Gaussian density has the following form [Prause (1999)]:

$$f_{GIG}(x;\lambda,\chi,\psi) = \frac{(\psi/\chi)^{\lambda/2}}{2K_\lambda\left(\sqrt{\psi\chi}\right)} x^{\lambda-1}\exp\left[-\frac{1}{2}\left(\chi x^{-1}+\psi x\right)\right], \quad x>0 \tag{2.25}$$

with $\lambda \epsilon \mathbb{R}$, $\chi = \delta^2$ and $\psi = \alpha^2 - \beta^2$.

The assumption under the Generalized Hyperbolic Model is that log returns are distributed as in Equation (2.22). The process for the log stock price under this assumption can be written as time changed Brownian Motion [Eberlein and Hammerstein (2004)]:

$$L_t = \mu t + \beta Y_t + B_{Y_t} \tag{2.26}$$

where $Y_t \sim GIG(\lambda, \delta, \alpha^2 - \beta^2)$ and B_t is Brownian Motion with zero drift and unit volatility.

The characteristic exponent for the Generalized Hyperbolic Distributions is [Prause (1999)]:

$$\psi(r) = \ln \left[\left(\frac{\alpha^2 - \beta^2}{\alpha^2 - (\beta + ir)^2} \right)^{\frac{\lambda}{2}} \frac{K_\lambda \left(\delta \sqrt{\alpha - (\beta + ir)^2} \right)}{K_\lambda \left(\delta \sqrt{\alpha^2 - \beta^2} \right)} \right] + ir\mu \tag{2.27}$$

from which the time evolution of the log return distribution can be obtained using Equation (2.2) and the Inverse Fourier Transform.

The Generalized Hyperbolic model allows for infinite activity and stochastic time change, which makes it more appropriate for the modeling of financial assets. Large jumps tend to occur at large values of Y_t and vice versa for small jumps. This model has as many parameters to estimate as Merton's Model, while allowing for a more complex processes.

2.5.1 Special Cases

There are two special cases of the General Hyperbolic Distribution commonly used in financial asset modeling, the Normal Inverse Gaussian Distribution and the Variance Gamma Distribution. The Normal Inverse Gaussian Distribution is the special case of Equation (2.22) where $\lambda = -\frac{1}{2}$ and the Variance Gamma Distribution is obtained by setting $\lambda > 0$ and $\delta = 0$ [Konlack Socgnia and Wilcox (2014)].

The Normal Inverse Gaussian Distribution can be written as a mean-variance normal mixture

where the mixing density is Inverse Gaussian, hence the name [Barndorff-Nielsen (1997)]. While the Variance Gamma Distribution can similarly be written as a mean-variance normal mixture with gamma mixing density [Madan and Seneta (1990)]. The shape of the Inverse Gaussian Density is similar to that of the Gamma Density, but the Inverse Gaussian Density has a sharper peak and greater skewness [Folks and Chhikara (1978)].

2.5.1.1 Normal Inverse Gaussian Process

The Normal Inverse Gaussian density function takes the form [Barndorff-Nielsen (1997)]:

$$f_{NIG}(x;\alpha,\beta,\mu,\delta) = a(\alpha,\beta,\mu,\delta)q\left(\frac{x-\mu}{\delta}\right)^{-1} K_1\left[\delta\alpha q\left(\frac{x-\mu}{\delta}\right)\right]\exp(\beta x) \tag{2.28}$$

with

$$a(\alpha,\beta,\mu,\delta) = \frac{\alpha}{\pi}\exp\left(\delta\sqrt{\alpha^2-\beta^2}-\beta\mu\right), \quad q(x) = \sqrt{1+x^2} \tag{2.29}$$

and K_1 a Bessel function of the third order and of index one. Now, the Normal Inverse Gaussian density can be written as a mean-variance mixture like in Equation (2.24):

$$f_{NIG}(x;\alpha,\beta,\mu,\delta) = \int_0^\infty f_{Norm}(x;\mu+\beta\omega,\omega)f_{IG}(\omega;\delta^2,\alpha^2-\beta^2)d\omega \tag{2.30}$$

where f_{IG} is an Inverse Gaussian density, which is obtained by setting $\lambda = -\frac{1}{2}$ in Equation (2.25).[8] The Inverse Gaussian density takes the form [Schoutens (2003)]:

$$f_{IG}(x;\chi,\psi) = \frac{\sqrt{\chi}}{\sqrt{2\pi}}x^{-\frac{3}{2}}\exp\left(\sqrt{\psi\chi}-\frac{1}{2}\left(\chi x^{-1}+\psi x\right)\right), \quad x>0 \tag{2.31}$$

where $\psi = \alpha^2-\beta^2$ and $\chi = \delta^2$.

[8] It follows from the following results: $K_{-\nu}(x) = K_\nu(x)$ and $K_{1/2} = \sqrt{\frac{\pi}{2}}x^{-1/2}\exp(-x)$ [Schoutens (2003)].

The Normal Inverse Gaussian process can be written as time changed Brownian Motion as follows [Barndorff-Nielsen (1997)]:

$$L_t = \mu t + \beta Y_t + B_{Y_t} \tag{2.32}$$

where Y_t is an Inverse Gaussian random variable, and B_t is Brownian Motion with zero drift and unit volatility.

The characteristic exponent takes the following form [Barndorff-Nielsen (1997)]:

$$\psi(r) = \delta \left[\sqrt{\alpha^2 - \beta^2} - \sqrt{\alpha - (\beta + ir)^2} \right]. \tag{2.33}$$

2.5.1.2 Variance Gamma Process

The Variance Gamma process is Brownian Motion with drift θ and volatility σ evaluated at random time. The subordinator is a Gamma process [Schoutens (2003)]:

$$L_t = \theta Y_t + \sigma B_{Y_t} \tag{2.34}$$

where $Y_{t+h} - Y_t$ has a $\Gamma\left(h/\nu, 1/\nu\right)$ distribution and thus a density of the form:

$$f_\Gamma(x) = \frac{\nu^{-h/\nu}}{\Gamma(h/\nu)} x^{h/\nu - 1} e^{-x/\nu}, \qquad x > 0 \tag{2.35}$$

with $\Gamma(x)$ a gamma function and $1/\nu > 0$. The density of L_t can be expressed as a mean-variance normal mixture with Gamma mixing density as follows [Madan *et al.* (1998)]:

$$f_{L_t}(x) = \int_0^\infty f_{Norm}\left(x; \theta g, \theta\sqrt{g}\right) \frac{g^{t/\nu - 1} \exp\left(-\frac{g}{\nu}\right)}{\nu^{t/\nu} \Gamma\left(\frac{t}{\nu}\right)} dg. \tag{2.36}$$

The characteristic exponent of the Variance Gamma process is:

$$\psi(r) = \left(\frac{1}{1 - i\theta\nu r + \left(\sigma^2 \nu / 2\right) r^2} \right)^{t/\nu}. \tag{2.37}$$

2.6 MEIXNER PROCESS

The Meixner density is defined as follows [Schoutens (2002)]:

$$f(x;\alpha,\beta,\delta) = \frac{(2\cos(\beta/2))^{2d}}{2\alpha\pi\Gamma(2d)} \exp\left[\frac{\beta x}{\alpha}\right] \left|\delta + \frac{ix}{\alpha}\right|^2 \tag{2.38}$$

where $\alpha > 0$, $-\pi < \beta < \pi$ and $\delta > 0$.

The characteristic function is:

$$\phi(r) = \left(\frac{\cos(\beta/2)}{\cosh\left(\frac{\alpha r - i\beta}{2}\right)}\right)^{2\beta} \exp(ir) \tag{2.39}$$

The Meixner process has no Brownian Motion part, it is purely a jump process $M = \{M_t,\ t \geq 0\}$, where $M_t \sim \text{Meixner}(\alpha, \beta, t\delta)$.

2.7 ADDING DRIFT

Some of the models described above; namely the Variance Gamma, Meixner and CGMY processes do not have a deterministic drift term. The drift can easily be added by introducing a new parameter μ. The new process will be identified by a $\sim$ and is defined as [Schoutens (2003)]:

$$\widetilde{L_t} \equiv \mu t + L_t. \tag{2.40}$$

The density becomes:

$$\widetilde{f}(x) = f(x - \mu). \tag{2.41}$$

The characteristic function becomes:

$$\widetilde{\phi}(r) = \phi(r)\exp(ir\mu). \tag{2.42}$$

The Lévy triplet becomes:

$$\widetilde{\gamma} = \gamma + \mu, \quad \widetilde{\sigma}^2 = \sigma^2, \quad \widetilde{\lambda}(dx) = \lambda(dx). \tag{2.43}$$

2.8 CONCLUSION

Stock market participants are continuously buying and selling stocks based on their market outlook. When new information is released, market participants make the appropriate adjustments in their outlook. The stochastic time change approach is useful in that when new information is being released rapidly - or when shocking information is released - the traded volume tends to increase and typically increases volatility. This corresponds to periods where the arrivals of large values of the subordinator are observed. When there is not much information - or low trading volume - there is typically less volatility and thus corresponds to periods where small observations of the subordinator are observed. Note, however, that stochastic time change models do not incorporate volatility clustering.

The Lévy process approach allows for the incorporation of fluctuations in market activity and thus fluctuations in volatility [Wu (2007)]. The results of Chapter 4 provide evidence that these time changed Brownian Motion models adequately describe the daily log return processes of the various South African indices considered, but only around the center of the data. The Lévy processes considered in Chapter 4 are the Generalized Hyperbolic process, the Variance Gamma process, the Normal Inverse Gaussian process and the Meixner process.

CHAPTER 3

QUANTUM MECHANICAL MODELS FOR LOG RETURN DISTRIBUTIONS

This chapter introduces the quantum mechanical models that will act as competitors to the Lévy models discussed in Chapter 2. The first section outlines the mathematics and the subsequent two sections describe the models. Section 4 concludes this chapter.

3.1 THE POSTULATES OF QUANTUM MECHANICS

Shankar (2012) describes the four postulates of quantum mechanics:

I The state of a quantum particle[1] is represented by a state vector $|\psi\rangle$ in Hilbert space.[2]

II Position and momentum in quantum mechanics are determined through Hermitian operators X and P, which act on the state vector $|\psi\rangle$ to give a probability amplitude.

III Given that a particle is in a state $|\psi\rangle$, the measurement of a particular variable corresponding to an operator Ω will yield an eigenvalue of Ω, say ω with probability $\mathbb{P}(\omega \,\epsilon\, [\omega, \omega + dx]) \propto |\langle\omega|\psi'\rangle|^2$ where $|\psi'\rangle = \Omega|\psi\rangle$. The observed quantity will then be fully deterministic as a result of the measurement,[3] for a brief period of time, after which the quantity will revert to a random (unknown) value. $\langle\omega|\psi'\rangle = \psi'(\omega)$ is called a probability amplitude.[4]

IV The state vector $|\psi\rangle$ obeys the Schrödinger equation:

$$i\hbar\frac{\partial}{\partial t}|\psi(t)\rangle = H|\psi(t)\rangle \tag{3.1}$$

where $H = -\frac{\hbar^2}{2m}\frac{\partial^2}{\partial x^2} + V(x,t)$ with $V(x,t)$ some potential function and $\hbar$ is Planck's reduced constant, with $\hbar = 1.0545718 \times 10^{-34}$.

In order to apply the mathematics of quantum mechanics to finance, there must be some justification for assuming that the above postulates hold in a financial setting.

[1] The quantum particle represents the log return on a stock index in this paper.
[2] Refer to Appendix B for a discussion on Dirac notation.
[3] This is called wave function collapse.
[4] $|\psi'(\omega)|^2$ is the probability density of ω.

The first postulate states that there exists some arbitrary function in Hilbert space from which all relevant observable quantities can be obtained.[5]

The second postulate is not relevant in this paper, it gives a quantum mechanical analog to position and momentum. In classical mechanics, position and momentum fully determine the state of a system [Shankar (2012)].

The third postulate states that the squared modulus of the state vector - transformed by the appropriate operator - gives the probability for the observable corresponding to the operator used. Once a measurement is taken, the pdf collapses to a deterministic point for a small period of time. Stock returns are traditionally considered random variables, and so to assume that the log returns can be described by a probability amplitude is not so far fetched. Furthermore, the collapse of the wave function is observed in financial markets when a trade is completed and a new price is set for the stock. Between trades, the stock price can be thought of as a random (unknown) quantity.

The fourth postulate specifies the time evolution of the probability amplitude. It seems to be a rather bold assumption, but as is shown in Section 3.1.1, it is not so far fetched that the Schrödinger equation is a useful starting point for modeling the log returns of stock prices.

3.1.1 Justifying the Schrödinger equation

As is discussed in Sakurai and Commins (1995), a time evolution operator, say $U(t)$, is required which will take the state function from time t_0 to time $T = t + t_0;\ t > 0$. More formally, $U(t)$ is required so that:

$$|\psi(T)\rangle = U(t)\,|\psi(t_0)\rangle\,. \tag{3.2}$$

Two useful properties of this time evolution operator would be:

1. The time evolution operator must be unitary, so that $|\psi(t_0)| = 1 \Rightarrow |\psi(T)| = 1$. This is

[5]The only observable quantity relevant in this paper is position, which corresponds to log return.

equivalent to requiring a time evolution operator that conserves probability.

2. The second property required is the composition property:

$$U(t_2) = U(t_2 - t_1)U(t_1) \tag{3.3}$$

with $t_0 \leq t_1 \leq t_2$.

Sakurai and Commins (1995) asserts that a choice of U that satisfies these properties is:

$$U(dt) = 1 - i\Omega dt \tag{3.4}$$

where Ω is Hermitian.

Property 1:[6]

$$U^{\dagger}(t)U(t) = \left(1 + i\Omega^{\dagger}dt\right)(1 - i\Omega dt) \tag{3.5}$$

$$= 1 + \Omega^2(dt)^2 \tag{3.6}$$

$$\approx 1 \text{ \{to the extent that terms of order } (dt)^2 \text{ and higher can be ignored.\}} \tag{3.7}$$

Thus, the time evolution operator in Equation (3.4) is unitary.

Property 2:

The operator specified in Equation (3.4) moves the state function forward in time by an infinitesimally small period of time. This can be extended to longer periods of time by iteratively moving forward. One key point to note is that Ω may be dependent on t_0, in which case it must be re-evaluated at each iterative step.

Now, a natural choice for Ω in the physical setting is the quantum Hamiltonian operator i.e. $\Omega = \frac{H}{\hbar}$. This stems from the Hamiltonian operator in classical mechanics [Sakurai and Commins (1995)].

[6]Refer to Appendix B for a discussion on the conjugate transpose - $U^{\dagger}$.

The Hamiltonian operator gives the total energy of a system, which is split into kinetic energy (KE) and potential energy (PE). KE gives the energy due to movement and PE gives the energy due to position. In the financial setting, one can think of energy as the total market activity. KE results from trading which causes changes in price, and PE is due to the current position along with information that has not yet been released [Lee (2020)]. Once information is released, it triggers a move in price that is based on what the current price is, and what market participants believe the price should be when the new information is taken into consideration. Furthermore, the potential function provides a mechanism for modelling mean reversion; if the returns move away from the mean, the potential part pushes the log returns back toward the equilibrium point [Ahn *et al.* (2018)].

In order to simplify the derivation, the time evolution operator starting at time t_0 and moving the state vector to time t will be denoted $U(t, t_0)$. Making use of the composition property:

$$U(t + dt, t_0) = U(t + dt, t)U(t, t_0) = \left(1 - \frac{iHdt}{\hbar}\right) U(t, t_0) \tag{3.8}$$

thus

$$i\hbar \frac{U(t + dt, t_0) - U(t, t_0)}{dt} = HU(t, t_0) \tag{3.9}$$

which can be rewritten as:

$$i\hbar \frac{\partial}{\partial t} U(t, t_0) = HU(t, t_0) \tag{3.10}$$

right-multiplying both sides by $|\psi\rangle$:

$$i\hbar \frac{\partial}{\partial t} U(t, t_0) |\psi\rangle = HU(t, t_0) |\psi\rangle . \tag{3.11}$$

Since the time evolution operator is on both sides of Equation (3.11), it is redundant and thus Equation (3.11) can be written as:

$$i\hbar\frac{\partial}{\partial t}\left|\psi\right\rangle = H\left|\psi\right\rangle \tag{3.12}$$

which is the Schrödinger equation.

Therefore, to allow the state vector for the return process of a financial asset to evolve according to the Schrödinger equation is to use a time evolution operator that conserves probability and satisfies the composition property. Then to allow the time evolution operator chosen to be governed by market activity to the extent that the modeling assumptions allow.

In both the Quantum Harmonic Oscillator and the Quantum An-Harmonic Oscillator, the data to which the respective distributions are fit is as follows:

$$x_t = L_t^* - \bar{L} \tag{3.13}$$

where $L_t^* = \ln\left(\frac{S_t}{S_{t-1}}\right)$, with S_t the stock price at the close of day t. $\bar{L}$ is the average log return over the period 01 January 2010 to 01 June 2020.

3.2 QUANTUM HARMONIC OSCILLATOR

The primary inspiration for this thesis is from Ahn *et al.* (2018). The paper describes how harmonic potential leads to a distribution that fits the return distribution of the FTSE All Share Index better than Brownian Motion and the Heston model.[7]

Consider first a Wiener Process W_t and the differential equation:

$$dx = v(x,t)dt + \sigma(x,t)W_t \tag{3.14}$$

[7]For a detailed discussion on the Heston model see Drăgulescu and Yakovenko (2002).

The Fokker Planck equation of (3.14) is provided below:[8]

$$\frac{\partial}{\partial t}\rho(x,t) = \frac{\partial^2}{\partial x^2}\left[D(x,t)\rho(x,t)\right] + \frac{\partial}{\partial x}\left[\rho(x,t)\frac{\partial V(x,t)}{\partial x}\right] \tag{3.15}$$

with $D(x,t) \equiv \frac{\sigma^2(x,t)}{2}$ and $V(x,t)$ some external potential that determines the drift such that $v(x,t) = \frac{-\partial V(x,t)}{\partial t}$.

Setting $D(x,t) = D$, with $D \,\epsilon\, \mathbb{R}$ and $V(x,t) = V(x)$ such that the external potential is independent of time, Equation (3.15) can be rewritten as:

$$\frac{\partial}{\partial t}\rho(x,t) = \left[\frac{\partial^2 V}{\partial x^2} + \frac{\partial V}{\partial x}\frac{\partial}{\partial x} + D\frac{\partial^2}{\partial x^2}\right]\rho(x,t) = \hat{L}\rho(x,t). \tag{3.16}$$

Equation (3.16) is difficult to solve due to $\hat{L}$ not being Hermitian.[9] Ahn *et al.* (2018) thus transforms Equation (3.16) into a time dependent Schrödinger equation so that the general solution of the Schrödinger equation can be used to obtain a solution for $\rho(x,t)$.

Firstly, a new function is introduced [Petroni *et al.* (1998)]:

$$\phi(x,t) \equiv \frac{\rho(x,t)}{\sqrt{\rho_s(x)}} \tag{3.17}$$

$\rho_s(x)$ is the stationary solution to Equation (3.15), and is given below [Putz (2019)]:

$$\rho_s(x) = \frac{1}{C}e^{-V(x)/D} \tag{3.18}$$

where C is a normalization constant given by $C \equiv \int_{-\infty}^{\infty} e^{-V(x)/D}dx$. With the appropriate algebraic manipulation, it can be shown that $\hat{L}\rho(x,t) = -\sqrt{\rho_s(x)}\hat{H}\phi(x,t)$, where:

$$\hat{H} = -\frac{1}{2}\frac{\partial^2 V}{\partial x^2} + \frac{1}{4D}\left(\frac{\partial V}{\partial x}\right)^2 - D\frac{\partial^2}{\partial x^2} \tag{3.19}$$

[8]The Fokker Planck equation gives a differential equation of the pdf from a differential equation of the underlying random variable. It is a similar result to the Kolmogorov forward equation. Refer to Risken and Frank (1996) for a discussion on the Fokker Planck equation.

[9]It follows intuitively that $\hat{L}$ is Non-Hermitian from the representation of $\frac{\partial}{\partial x}$ as a square matrix using the finite difference method.

Then, by making the substitution $\tau = -i\hbar t$, the Fokker Planck Equation - Equation (3.16) - can be written as a time dependent Schrödinger equation:

$$i\hbar\frac{\partial}{\partial\tau}\phi(x,\tau) = \hat{H}\phi(x,\tau) = -\frac{\hbar^2}{2m}\frac{\partial^2}{\partial x^2}\phi(x,\tau) + U(x)\phi(x,\tau) \tag{3.20}$$

where $m \equiv \frac{\hbar^2}{2D}$ and the effective potential $U(x)$ is:

$$U(x) \equiv -\frac{1}{2}\frac{\partial^2 V(x)}{\partial x^2} + \frac{1}{4D}\left[\frac{\partial V(x)}{\partial x}\right]^2. \tag{3.21}$$

Now, the time independent Schrödinger[10] equation is [Shankar (2012)]:

$$\hat{H}\phi(x) = E\phi(x) \tag{3.22}$$

Equation (3.22) has countably infinite solutions, where the n'th solution is the n'th eigenfunction of $\hat{H}$ and is denoted $\phi_n(x)$. The n'th eigenvalue is denoted E_n, and the general solution is a linear combination of the eigenfunctions [Agarwal and O'Regan (2008)]:

$$\phi(x) = \sum_{n=0}^{\infty} A_n\phi_n(x) \tag{3.23}$$

The time evolution operator is $e^{-\frac{i}{\hbar}E_n\tau}$, and so the general solution to Equation (3.19) is obtained as [Ahn *et al.* (2018)]:

$$\phi(x,\tau) = \sum_{n=0}^{\infty} A_n\phi_n(x)\exp\left(-\frac{i}{\hbar}E_n\tau\right) \tag{3.24}$$

The A_n's are called the amplitudes of the normalized solutions to Equation (3.22), and are given as [Ahn *et al.* (2018)]:

$$A_n = \int_{-\infty}^{\infty}\frac{\phi_n(x)}{\sqrt{\rho_s(x)}}\rho(x,0)dx \tag{3.25}$$

[10]Note the similarity of Equation (3.22) to the eigenvalue problem in linear algebra.

Now, taking the Taylor expansion of $U(x)$ around 0 gives:

$$U(x) = \sum_{n=0}^{\infty} \frac{1}{n!} \frac{d^n U(x)}{dx^n}\bigg|_0 \tag{3.26}$$

Ignoring the higher order terms:

$$U(x) \approx U(0) + \frac{1}{2}kx^2 \tag{3.27}$$

with $k \equiv \frac{d^2U(x)}{dx^2}\Big|_0$.

In classical mechanics, the harmonic oscillator describes a pendulum.[11] $F \equiv -\frac{dU}{dx} = k^*x$ is the restoring force which pushes a pendulum currently not in the equilibrium position back to equilibrium. $\omega \equiv \sqrt{k^*/m}$ gives the angular frequency which determines how quickly the pendulum oscillates. The quantum harmonic oscillator functions in a similar way, the difference being that the quantum harmonic oscillator is random in nature, which seems ideal for modelling log return series with mean reversion.

Taking $V(x) = \gamma x^2$ gives the harmonic form of the effective potential:

$$U(x) = -\gamma + \frac{1}{2}m\omega^2 x^2 \tag{3.28}$$

with $\gamma = \omega\sqrt{mD/2}$.

It is well known in physics literature that the n'th eigenfunction of the Hamiltonian with harmonic potential is [Ahn *et al.* (2018)]:

$$\phi_n(x) = \frac{1}{\sqrt{2^n n!}} \left(\frac{m\omega}{\pi\hbar}\right)^{1/4} H_n\left(\sqrt{\frac{m\omega}{\hbar}}x\right) \exp\left(-\frac{m\omega}{2\hbar}x^2\right) \tag{3.29}$$

where $H_n(x)$ is the n'th physicists Hermite polynomial. $H_n(x) = \frac{n!}{2\pi i} \oint e^{-t^2+2tx} t^{-n-1} dt$. $H_0(x) = 1$, $H_1(x) = 2x$, $H_2(x) = 4x^2 - 2$, ... [Weisstein (2020*b*)].

[11] The harmonic oscillator also describes other physical phenomena, such as a weight on a spring.

The corresponding eigenenergy is:

$$E_n = n\hbar\omega \tag{3.30}$$

The Fokker Planck equation - Equation (3.14) - can then be solved:

$$\rho(x,t) = \sum_{n=0}^{\infty} \frac{A_n}{\sqrt{2^n n!}} \sqrt{\frac{m\omega}{\pi\hbar}} \exp\left(-E_n t\right) H_n\left(\sqrt{\frac{m\omega}{\hbar}}x\right) \exp\left(-\frac{m\omega}{\hbar}x^2\right) \tag{3.31}$$

The stationary solution in Equation (3.17) - $\rho_s(x)$ - is given as:

$$\rho_s(x) = \sqrt{\frac{m\omega}{\pi\hbar}} \exp\left(-\frac{m\omega}{\hbar}x^2\right) \tag{3.32}$$

Equation (3.31) can then be written as a mixed χ distribution:[12]

$$\rho(x,t) = \sum_{n=0}^{\infty} C_n(t) p_n(x) \tag{3.33}$$

where $C_n(t) = \left(A_n/\sqrt{2^n n!}\right)\sqrt{m\omega/\pi\hbar}e^{E_n t}$ and $p_n(x) = H_n\left(\sqrt{m\omega/\hbar}x\right)e^{-(m\omega/\hbar)x^2}$.

Ahn *et al.* (2018) claims that the goodness of fit comes from the incorporation of market uncertainty and a mean reverting force. Chapter 4 investigates this claim and shows that the Quntum Harmonic Oscillator performs poorly compared to the other models considered. This is potentially due to approximating $\rho(x,t)$ as:

$$\rho(x,t) \approx \sum_{n=0}^{4} C_n(t) p_n(x) \tag{3.34}$$

for the practical application of the model.

To estimate the $m\omega$ parameter of the Quantum Harmonic Oscillator, consider the ground state

[12] A χ random variable Y is defined as $Y = \sqrt{X}$, where $X \sim \chi^2$, see Weisstein (2020*a*).

where $H_0(x) = 1$:

$$p_0(x) = e^{-\left(\frac{m\omega}{\hbar}\right)x^2} \tag{3.35}$$

Note the similarity to the density function of a Gaussian random variable with mean zero and variance σ^2 given below:

$$f(x) \propto e^{-\frac{1}{2}\frac{x^2}{\sigma^2}} \tag{3.36}$$

$C_n(t)$ is a normalizing constant, and the MLE of $m\omega$ is obtained by comparing the parameters in Equation (3.35) and Equation (3.36):

$$\hat{m\omega} = \frac{\hbar}{2\hat{\sigma}^2} \tag{3.37}$$

where σ^2 is the variance of log returns and $\hbar$ is the reduced Planck's constant. The MLE of σ^2 in a $N(0, \sigma^2)$ distribution is given below [Rice (2006)]:

$$\hat{\sigma}^2 = \frac{1}{n}\sum_{i=1}^{n} x_i^2 \tag{3.38}$$

with x_i, $i = 1, 2, 3, ..., n$ the mean centered log returns.

Once $\hat{m\omega}$ is obtained, the constants $C_0(t), C_1(t), ..., C_4(t)$ are estimated by minimizing the Cramer-von Mises goodness of fit metric:

$$CVM = \frac{1}{12N} + \sum_{i=1}^{N}\left[\frac{i - 0.5}{N} - F(x_i)\right]^2 \tag{3.39}$$

where x_i, $i \in \{1, 2, 3, ..., N\}$ is the i'th ordered log return from a set with N observations and F is the specific hypothesised distribution, with $C_5(t), C_6(t), ...$ all assumed to be zero.

Using the appropriate transformations, a probability density for the log return has been derived from a Brownian Motion process with constant volatility and drift dependent the log return. The drift is related to the derivative of the harmonic potential function, which is parabolic, and thus

incorporates mean reversion.

3.3 QUANTUM AN-HARMONIC OSCILLATOR

A quantum mechanical model for the stock market is derived from supply and demand in Lee (2020). This section provides an overview of this derivation along with a brief discussion on solving the resulting Schrödinger equation. A similar derivation can be found in Gao and Chen (2017).

Firstly, instantaneous supply and demand at time t are denoted $z_+(t)$ and $z_-(t)$ respectively. Then the excess demand at time t is defined as:

$$\Delta z(t) = z_+(t) - z_-(t) \tag{3.40}$$

Gao and Chen (2017) describes the relationship between $r(t)$ and $\Delta z(t)$ as:

$$r(t) = \frac{\Delta z(t)}{\gamma} \tag{3.41}$$

with γ a measure of market depth i.e. how much excess demand is required to move the price.

The derivative of instantaneous return with respect to time is:

$$\frac{dr(t)}{dt} = \frac{d^2p(t)}{dt^2} = \frac{1}{\gamma}\frac{d\Delta z(t)}{dt} \tag{3.42}$$

An algebraic form of $\frac{d\Delta z(t)}{dt}$ is obtained through the action of various market participants. According to Lee (2020), the primary market participants in secondary financial markets are market makers, arbitrageurs, hedgers, speculators and investors. The dynamics of these participants are outlined in the next subsection.

3.3.1 Dynamics of Market Participants

3.3.1.1 Market Makers

The role of the market makers is to absorb excess buy and sell orders. The dynamics of these participants is assumed to be:

$$\begin{aligned} \left.\frac{dz_+(t)}{dt}\right|_{\text{MM}} &= -\alpha_+ z_+(t) \\ \left.\frac{dz_-(t)}{dt}\right|_{\text{MM}} &= -\alpha_- z_-(t) \end{aligned} \tag{3.43}$$

with α_+ and α_- measures of the market makers' collective absorption ability. The dynamics of excess demand is then give by:

$$\begin{aligned} \left.\frac{d\Delta z(t)}{dt}\right|_{\text{MM}} &= \left.\frac{d(z_+(t) - z_-(t))}{dt}\right|_{\text{MM}} \\ &= -\alpha_+ z_+(t) + \alpha_- z_-(t) \end{aligned} \tag{3.44}$$

Assuming $\alpha_- = \alpha_+ = \alpha_{\text{MM}}$:

$$\left.\frac{d\Delta z(t)}{dt}\right|_{\text{MM}} = -\gamma \alpha_{\text{MM}} r(t) \tag{3.45}$$

3.3.1.2 Arbitrageurs

Arbitrageurs take advantage of price mismatches in secondary financial markets. The prevailing theory is that arbitrageurs identify these mismatches and execute the necessary trades fast enough, so that the time periods in which price mismatches exist are negligibly short [Hull (2009)]. The no arbitrage principle is crucial for determining the fair prices of financial derivatives.

3.3.1.3 Speculators

Speculators engage in risky financial transactions in an attempt to profit from short term price fluctuations. Since they do not necessarily consider the risks involved in their trades, their dynamics

are assumed to be:

$$\left.\frac{d\Delta z(t)}{dt}\right|_{\mathrm{SP}} = -\delta_{\mathrm{SP}} r(t) \tag{3.46}$$

where the δ_{SP} term relates the instantaneous return observed to instantaneous changes in the excess demand of speculators.

3.3.1.4 Hedgers

Hedgers apply various trading strategies to their portfolio to mitigate market risks. Hedging strategies are designed to offset the profit and loss of a security or portfolio of securities resulting in reduced net price movements. Their dynamics are assumed to be:

$$\left.\frac{d\Delta z(t)}{dt}\right|_{\mathrm{HG}} = -(\delta_{\mathrm{HG}} - \nu_{\mathrm{HG}} r^2(t)) r(t), \tag{3.47}$$

the ν_{HG} term is a measure of control over market volatility and the δ_{HG} term relates the instantaneous return to the number of orders placed[13].

3.3.1.5 Investors

Investors are market participants who act with a degree of risk control when placing orders. Investors are similar to speculators in that they are attempting to profit from changes in market price, but typically over a longer time frame and with more consideration of the risk involved. Their dynamics are assumed to be:

$$\left.\frac{d\Delta z(t)}{dt}\right|_{\mathrm{IV}} = [\delta_{\mathrm{IV}} - \nu_{\mathrm{IV}} r^2(t)] r(t) \tag{3.48}$$

[13]The difference between the quantity of buy and sell orders is what influences excess demand.

3.3.2 Deriving the Quantum Finance Schrödinger Equation (QFSE)

Combining the dynamics of the market participants described above gives:

$$\begin{aligned}\frac{d\Delta z(t)}{dt} &= \frac{d\Delta z(t)}{dt}\bigg|_{\text{MM}} + \frac{d\Delta z(t)}{dt}\bigg|_{\text{SP}} + \frac{d\Delta z(t)}{dt}\bigg|_{\text{HG}} + \frac{d\Delta z(t)}{dt}\bigg|_{\text{IV}} \\ &= -\delta r(t) + \nu r^3(t) \end{aligned} \tag{3.49}$$

Then, with $\gamma^* = \frac{1}{\gamma}$:

$$\frac{dr(t)}{dt} = \gamma^* \frac{d\Delta z(t)}{dt} = -\gamma^* \delta r(t) + \gamma^* \nu r^3(t) \tag{3.50}$$

These price dynamics will be used in the Langevin representation of Brownian Motion to determine the potential. The Langevin representation of Brownian Motion is [Lee (2020)]:

$$m_r \frac{d^2 r(t)}{dt^2} = -\eta \frac{dr(t)}{dt} - \frac{dU(r)}{dr} \tag{3.51}$$

with m_r the mass of the financial particle,[14] η is a damping force factor and $U(r)$ is the time-independent potential as in Section 3.2.

For consistency between Equation (3.50) and Equation (3.51); Lee (2020) considers the overdamping condition - where $m_r \frac{d^2 r(t)}{dt^2} = 0$ - which then gives:

$$\frac{dU(r)}{dr} = \eta \frac{dr(t)}{dt} = -\gamma^* \eta \delta r(t) + \gamma^* \eta \nu r^3 \tag{3.52}$$

Solving for the potential gives:

$$U(r) = \frac{\gamma^* \eta \delta}{2} r^2(t) - \frac{\gamma^* \eta \nu}{4} r^4(t) \tag{3.53}$$

Substituting the potential obtained in Equation (3.53) as $V(x,t) = U(r)$ in the Schrödinger equation - Equation (3.1) - then gives what Lee (2020) refers to as the Quantum Finance Schrödinger

[14] The mass represents characteristics unique to the security such as market capitalization [Lee (2020)].

Equation (QFSE):[15]

$$\left[\frac{-\hbar}{2m}\frac{d^2}{dr^2} + \left(\frac{\gamma^*\eta\delta}{2}r^2 + \frac{\gamma^*\eta\nu}{4}r^4\right)\right]\psi(r) = E\psi(r) \tag{3.54}$$

Now, to find the pdf of the above process, one must solve for $\psi(r)$. The next section provides a discussion on numerical methods that can be used to find an approximate solution to the QFSE.

3.3.3 Numerical Approximation to Solve the QFSE

To obtain an approximate solution to Equation (3.54), a grid is specified for r, in this case the grid is the vector $\boldsymbol{r}^T = (-0.15, -0.1499, -0.1498, ..., 0.1498, 0.1499, 0.15)$. Now, $\psi(\boldsymbol{r})$, can be expressed as a vector with 3001 elements.

LeVeque (2007) shows how a second order differential operator can be written as a square matrix using the finite difference technique:[16]

$$\frac{d^2}{dr^2} \approx \frac{1}{h^2}\begin{bmatrix} -2 & 1 & 0 & 0 & ... & 0 \\ 1 & -2 & 1 & 0 & ... & 0 \\ 0 & 1 & -2 & 1 & ... & 0 \\ 0 & 0 & 1 & -2 & ... & 0 \\ \vdots & \vdots & \vdots & \vdots & \ddots & \vdots \\ 0 & 0 & 0 & 0 & ... & -2 \end{bmatrix} \tag{3.55}$$

where $h = 0.0001$ is the grid spacing used to define the vector $\boldsymbol{r}$.

To simplify the estimation procedure, set $\frac{\gamma^*\eta\delta}{2} = \alpha$ and $\frac{\gamma^*\eta\nu}{4} = \beta$. Call the matrix in Equation (3.55) $\boldsymbol{D}$, so that (3.54) can be expressed as:

$$\left[\frac{-\hbar}{2m}\boldsymbol{D} + \alpha\boldsymbol{R^2} + \beta\boldsymbol{R^4}\right]\psi(\boldsymbol{r}) = E\psi(\boldsymbol{r}) \tag{3.56}$$

[15] Note that E is a scalar, and solving the QFSE is analogous to the eigenvalue problem in linear algebra.

[16] In the finite difference method, $\frac{d^2\psi(r)}{dr^2} \approx \frac{\psi(r_{i+1}) - 2\psi(r_i) + \psi(r_{i-1})}{h^2}$.

$\boldsymbol{R^2}$ is a matrix with $\boldsymbol{r}^2 = [r_1^2, r_2^2, ..., r_N^2]^T$ along the main diagonal and zeros elsewhere. Similarly, $\boldsymbol{R}^4$ is a diagonal matrix where the main diagonal is $\boldsymbol{r}^4 = [r_1^4, r_2^4, ..., r_N^4]^T$.

The general solution to Equation (3.54) is then some linear combination[17] of the eigenvectors of the matrix:

$$\left[\frac{-\hbar}{2m}\boldsymbol{D} + \alpha\boldsymbol{R^2} + \beta\boldsymbol{R^4}\right] \tag{3.57}$$

i.e. $\psi(\boldsymbol{r}) = C_0\boldsymbol{\psi_0} + C_1\boldsymbol{\psi_1} + C_2\boldsymbol{\psi_2} + ...$ where $\boldsymbol{\psi_0}$ is the eigenvector corresonding to the smallest eigenvalue, $\boldsymbol{\psi_1}$ is the eigenvector corresponding to the second smallest eigenvalue etc.

To simplify computation, only the eigenvectors corresponding to the five smallest eignevalues are used.[18] $\boldsymbol{\psi_0}$ is called the ground state. Using the ground state: m, α and β are estimated using MLE, where the observed returns are binned to the closest value in $\boldsymbol{r}$. Then C_0, C_1, C_2, C_3 and C_4 are estimated by minimizing the Cramer-von Mises goodness of fit statistic:

$$CVM = \frac{1}{12N} + \sum_{i=1}^{N}\left[\frac{i-0.5}{N} - F(x_i)\right]^2 \tag{3.58}$$

where x_i is the i'th ordered log return from a set of N observations and F is the specific hypothesised distribution, with $C_5, C_6, ...$ all assumed to be zero.

3.4 CONCLUSION

The quantum models provide an interesting framework to think of uncertainty in financial markets. Since all assets are traded by multiple parties, who all have unique outlooks on the economy, the stock price is always in a superposition between all outlooks until it is traded and a price measurement is taken.

Section 3.3 describes the dynamics of demand and supply for the various types of market participants. The QFSE is then developed from these dynamics. While the theory is interesting and

[17] In physics literature, this linear combination is referred to as a superposition.
[18] This corresponds to the five lowest energy levels.

it seems promising to take a ground up approach to building a model for the dynamics of stock price returns, it is very difficult to implement this model in practice.

Both models provided in this chapter use approximate solutions to their respective Schrödinger equations. Obtaining these approximate solutions is computationally expensive and Chapter 4 shows that they yield results that are not as well suited to the log returns of stocks as the Lévy models from Chapter 2.

CHAPTER 4

EMPIRICAL RESULTS

In this chapter, the models are fit to various JSE indices using the methodologies discussed above and a discussion on the goodness of fit of the various models is provided. The first section considers the Lévy models. The second section is concerned with the Quantum Mechanical models.

For each of the models considered, a histogram of the data is plotted with the theoretical density overlain. Then the Q-Q and P-P Plots are provided. Finally, a hypothesis test based on the Kolmogorov-Smirnov goodness of fit statistic is provided. The Kolmogorov-Smirnov test statistic is defined as [Murphy (1968)]:

$$D = \max_{1 \leq i \leq N} \left(F(x_i) - \frac{i-1}{N}, \frac{i}{N} - F(x_i) \right) \tag{4.1}$$

where x_i is the i'th ordered log return and $F(x_i)$ is the specific hypothesised distribution. The null hypothesis is that the data follows the hypothesised distribution, and is rejected if D is larger than the critical value corresponding to a significance level of α.[1]

The data used for this empirical study was obtained from *investing.com* using the *investpy* Application Programming Interface (API) in Python. Daily closing prices on the JSE Top 40 Index, JSE SWIX, JSE Banks Index, JSE Resources Index, JSE Industrials Index and the JSE Financials Index for the period 01 January 2010 to 01 June 2020 are used to compute daily log returns. The time period considered contains various crashes in financial markets, which tests how well the models considered capture tail events.

[1] In this paper, α is taken to be 0.1.

4.1 LÉVY MODELS

4.1.1 Generalized Hyperbolic

The theoretical densities of the Generalized Hyperbolic process is overlain on the respective histograms below.

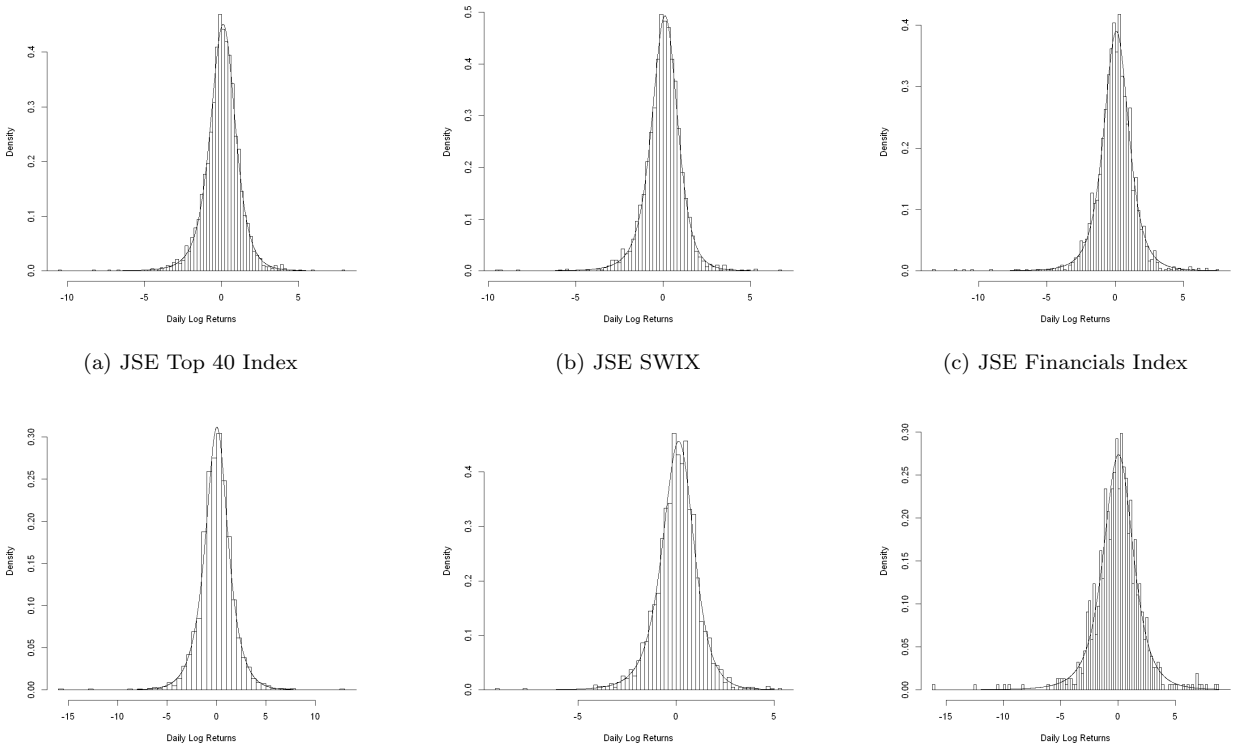

(a) JSE Top 40 Index (b) JSE SWIX (c) JSE Financials Index

(d) JSE Resources Index (e) JSE Industrials Index (f) JSE Banks Index

Figure 4.1: Generalized Hyperbolic Density Plots

Q-Q Plots of the Generalized Hyperbolic process are provided below.

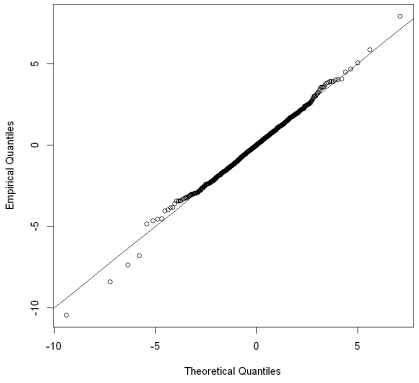

(a) JSE Top 40 Index

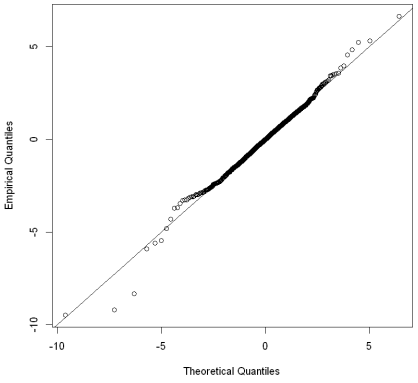

(b) JSE SWIX

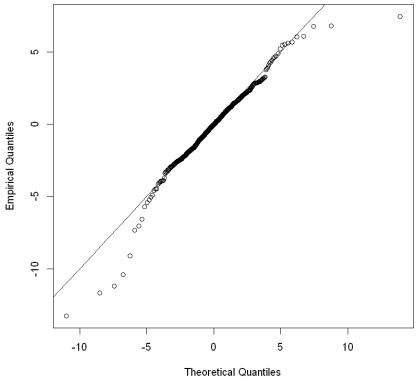

(c) JSE Financials Index

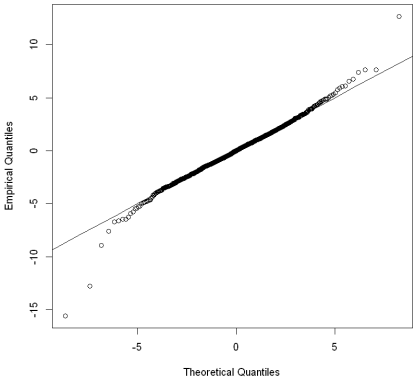

(d) JSE Resources Index

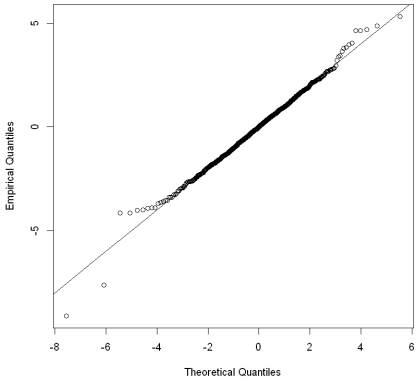

(e) JSE Industrials Index

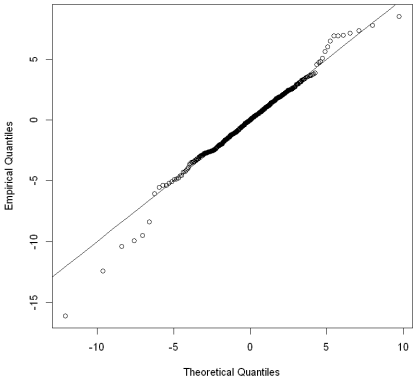

(f) JSE Banks Index

Figure 4.2: Generalized Hyperbolic Q-Q Plots

P-P Plots of the Generalized Hyperbolic process are provided below.

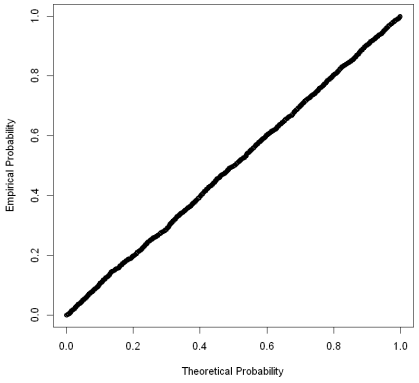

(a) JSE Top 40 Index

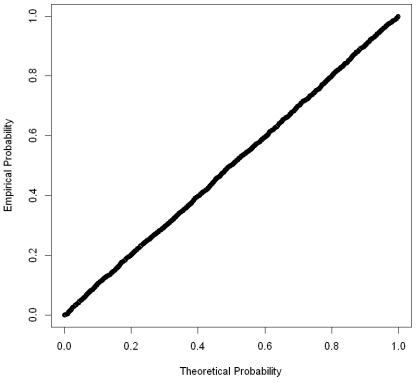

(b) JSE SWIX

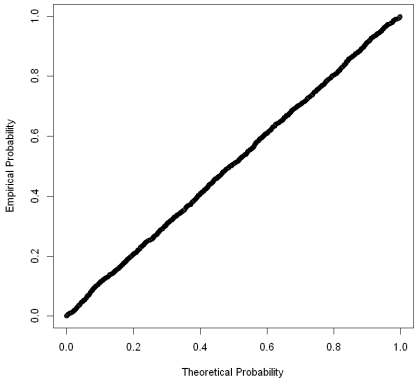

(c) JSE Financials Index

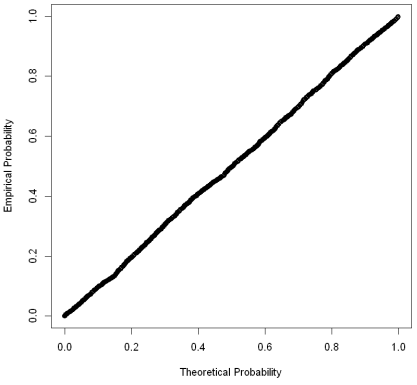

(d) JSE Resources Index

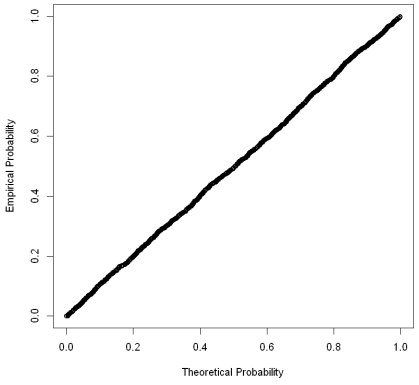

(e) JSE Industrials Index

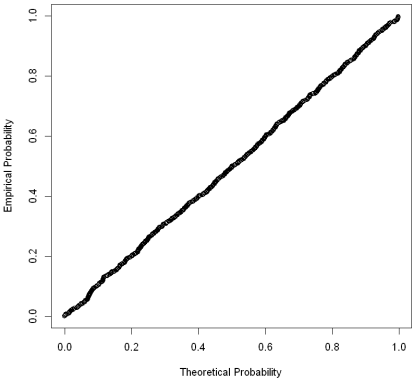

(f) JSE Banks Index

Figure 4.3: Generalized Hyperbolic P-P Plots

Table 4.1: Generalized Hyperbolic Distribution Parameter Estimates

	λ	α	β	δ	μ
JSE Top 40	-2.062	0.179	-0.088	1.697	0.138
JSE SWIX	-2.066	0.174	-0.130	1.548	0.165
JSE Financials	-1.781	0.015	-0.015	1.801	0.090
JSE Resources	0.419	0.854	-0.024	1.243	0.058
JSE Industrials	-1.762	0.538	-0.150	1.610	0.219
JSE Banks	-1.669	0.048	-0.028	2.478	0.073

Table 4.2: Kolmogorov-Smirnov Fit Statistics for the Generalized Hyperbolic Process

	D-Statistic	p-value
JSE Top 40	0.012	0.9893
JSE SWIX	0.007	1
JSE Financials	0.015	0.9603
JSE Resources	0.016	0.9494
JSE Industrials	0.016	0.9993
JSE Banks	0.015	1

4.1.1.1 Discussion

From the density and P-P plots it is clear that the Generalized Hyperbolic model works well as a model for daily log returns. Considering the KS statistics, there is no statistical evidence to reject the null hypothesis that daily log returns are generated by the Generalized Hyperbolic process, however the Q-Q plots allude to an underestimation of the frequency of tail events. One should therefore be careful when using the Generalized Hyperbolic process for tail applications such as Value at Risk due to the weakness in capturing extreme events.

4.1.2 Normal Inverse Gaussian Process

The theoretical densities of the Normal Inverse Gaussian process is overlain on the respective histograms below.

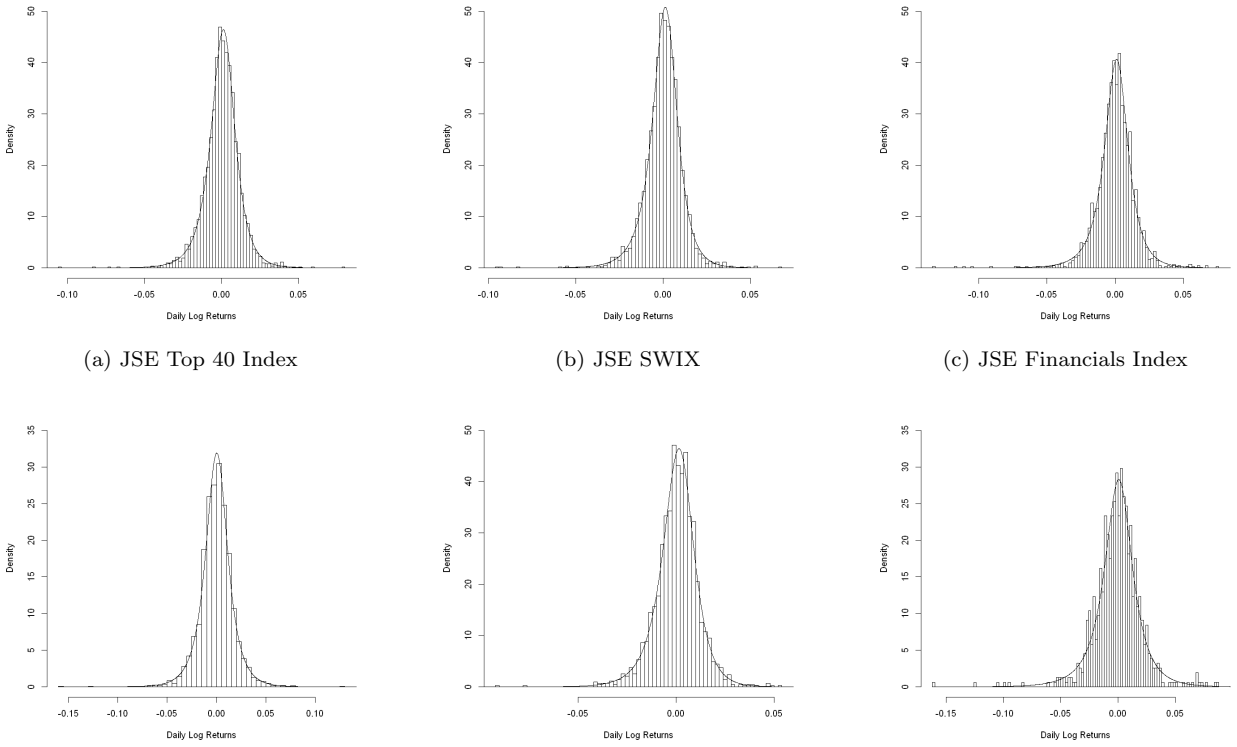

(a) JSE Top 40 Index (b) JSE SWIX (c) JSE Financials Index

(d) JSE Resources Index (e) JSE Industrials Index (f) JSE Banks Index

Figure 4.4: Normal Inverse Gaussian Density Plots

Q-Q Plots of the Normal Inverse Gaussian process are provided below.

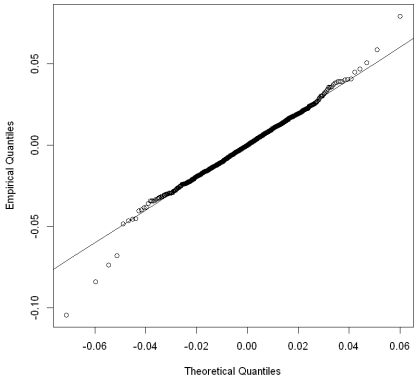

(a) JSE Top 40 Index

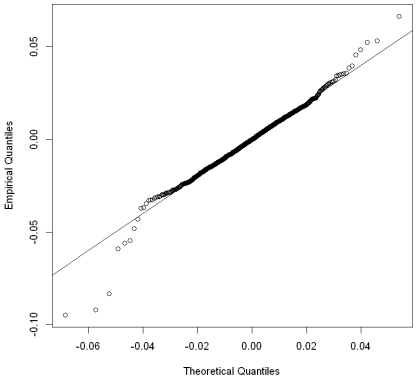

(b) JSE SWIX

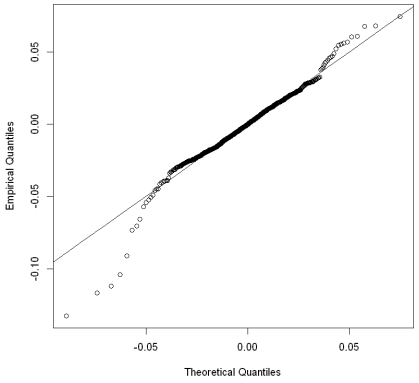

(c) JSE Financials Index

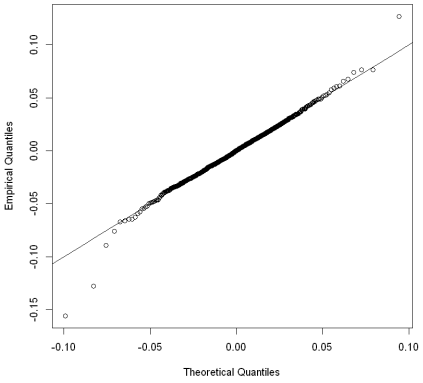

(d) JSE Resources Index

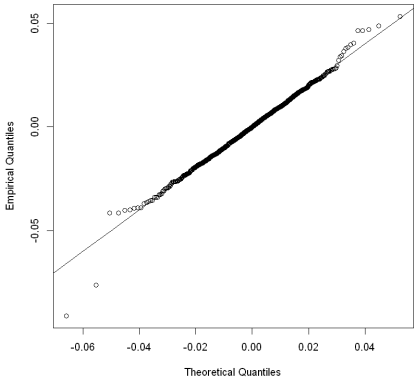

(e) JSE Industrials Index

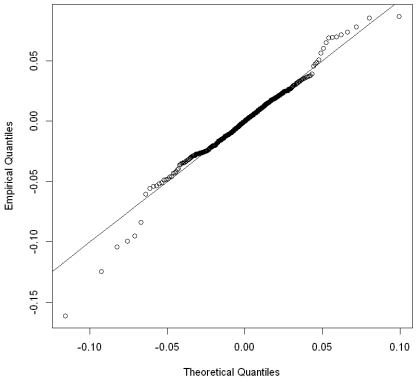

(f) JSE Banks Index

Figure 4.5: Normal Inverse Gaussian Q-Q Plots

P-P Plots of the Normal Inverse Gaussian process are provided below.

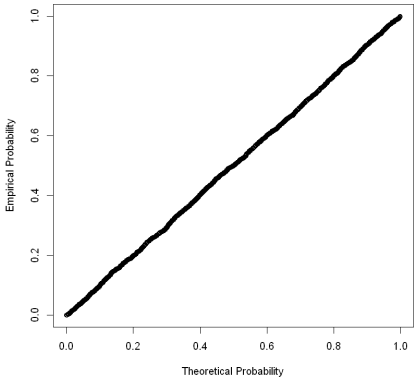

(a) JSE Top 40 Index

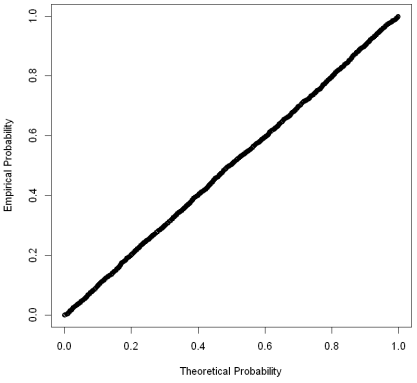

(b) JSE SWIX

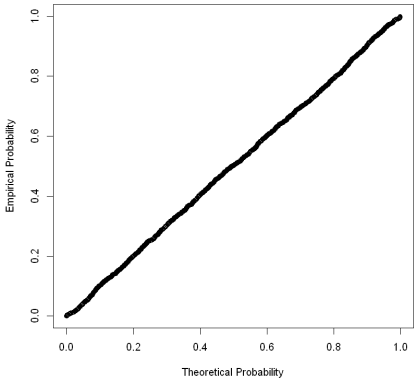

(c) JSE Financials Index

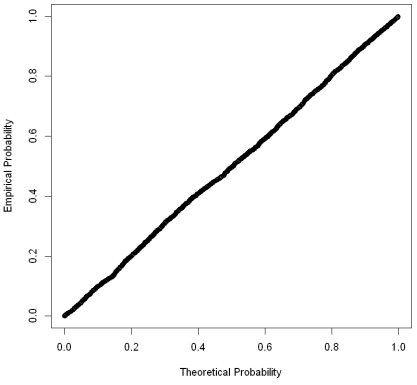

(d) JSE Resources Index

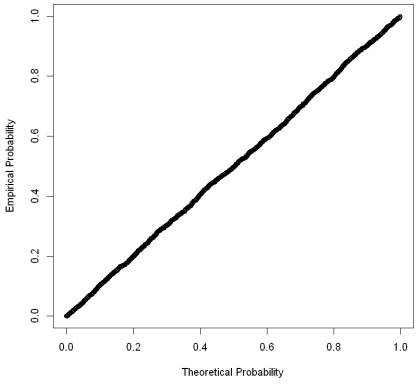

(e) JSE Industrials Index

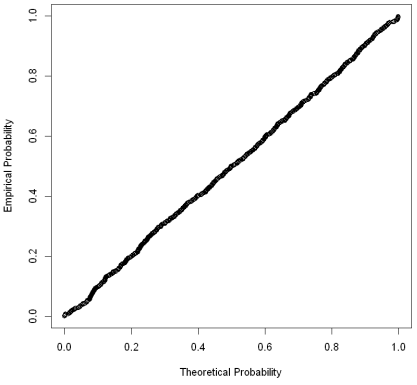

(f) JSE Banks Index

Figure 4.6: Normal Inverse Gaussian P-P Plots

Table 4.3: Normal Inverse Gaussian Distribution Parameter Estimates

	α	β	δ	μ
JSE Top 40	88.250	-10.046	0.011	0.002
JSE SWIX	94.993	-14.926	0.010	0.002
JSE Financials	64.302	-7.079	0.012	0.001
JSE Resources	56.096	-1.660	0.016	0.0004
JSE Industrials	0.012	101.454	-16.308	0.002
JSE Banks	0.016	39.374	-3.647	0.001

Table 4.4: Kolmogorov-Smirnov Fit Statistics for the Normal Inverse Gaussian Process

	D-Statistic	p-value
JSE Top 40	0.009	0.9999
JSE SWIX	0.009	1
JSE Financials	0.011	0.9993
JSE Resources	0.013	0.9956
JSE Industrials	0.011	0.9993
JSE Banks	0.018	0.9986

4.1.2.1 Discussion

The Normal Inverse Gaussian distribution performs just as well as the Generalized Hyperbolic process across all metrics considered, while using fewer parameters. Once again there is no statistical evidence to reject the null hypothesis that the daily log returns are generated by the Normal Inverse Gaussian process. The p-values are generally larger in the case of the Normal Inverse Gaussian process, thus suggesting that the model provides a better fit. The Q-Q plots for the Normal Inverse Gaussian model, however, suggest that the Normal Inverse Gaussian model underestimates the probabilities in the tails of the log return data. The poor performance in the tails should be considered in practical applications of the Normal Inverse Gaussian model, particularly in applications concerned with extreme events.

4.1.3 Variance Gamma Process

The theoretical densities of the Variance Gamma process is overlain on the respective histograms below.

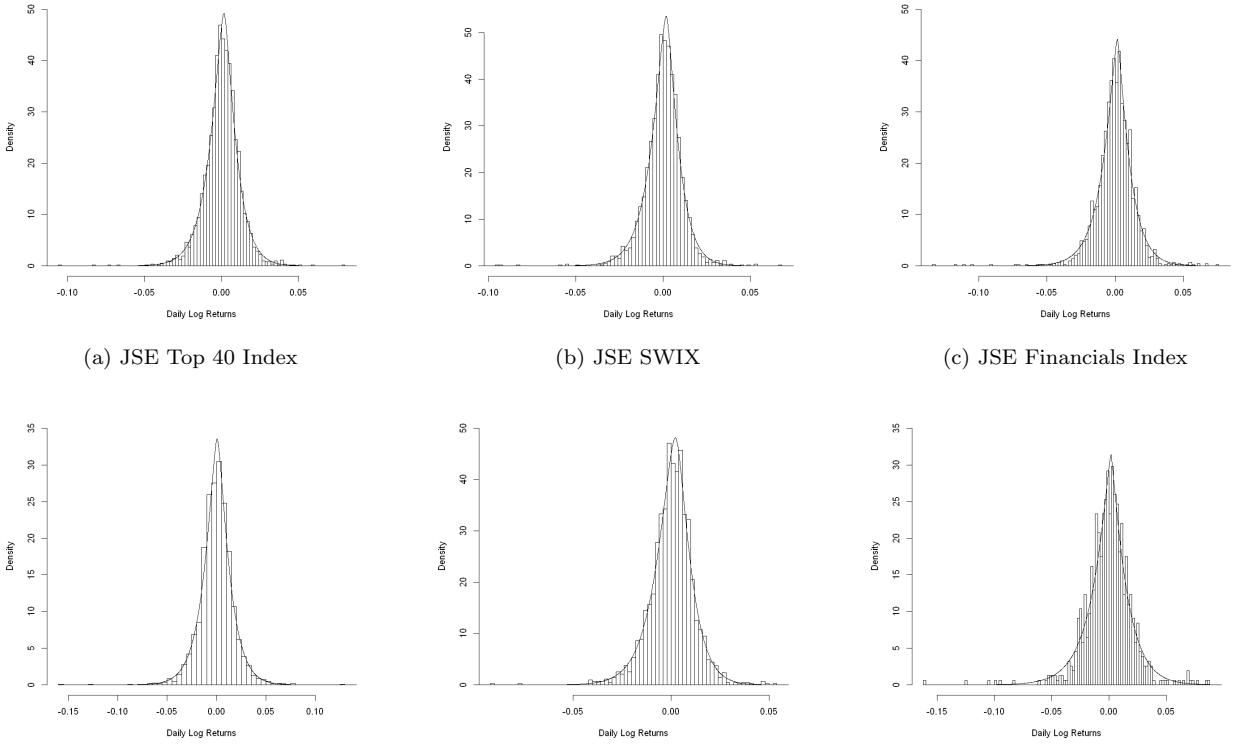

(a) JSE Top 40 Index (b) JSE SWIX (c) JSE Financials Index

(d) JSE Resources Index (e) JSE Industrials Index (f) JSE Banks Index

Figure 4.7: Variance Gamma Density Plots

Q-Q Plots of the Variance Gamma process are provided below.

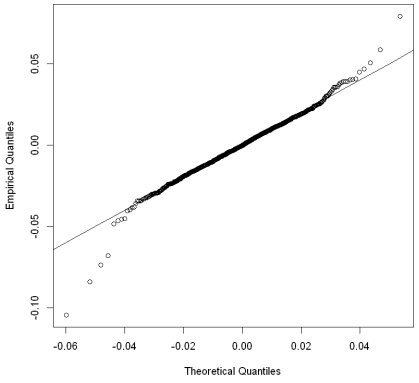

(a) JSE Top 40 Index

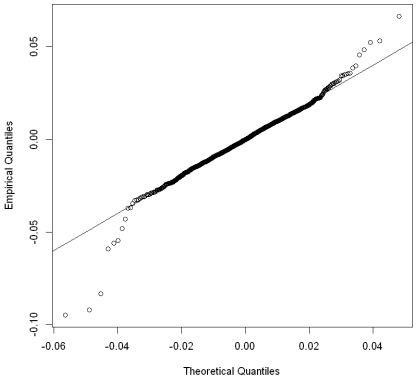

(b) JSE SWIX

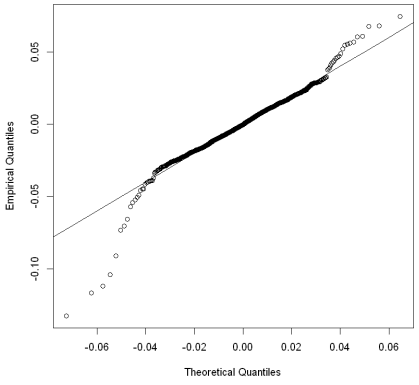

(c) JSE Financials Index

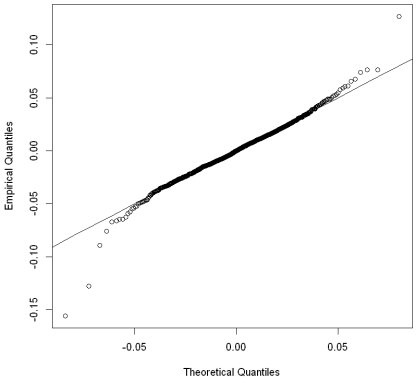

(d) JSE Resources Index

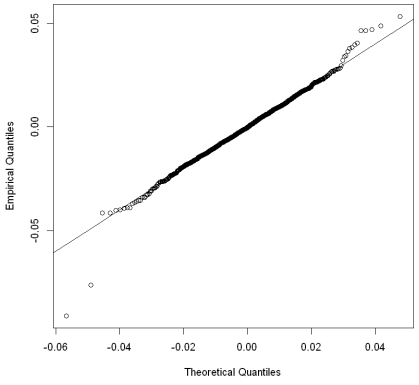

(e) JSE Industrials Index

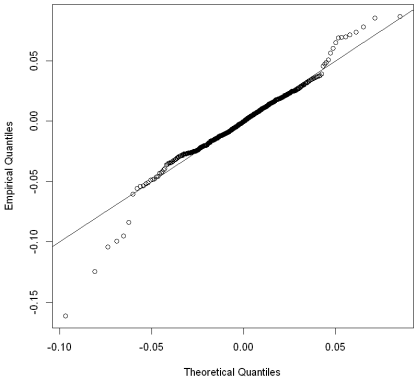

(f) JSE Banks Index

Figure 4.8: Variance Gamma Q-Q Plots

P-P Plots of the Variance Gamma process are provided below.

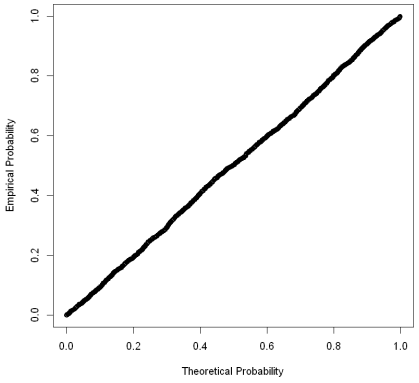

(a) JSE Top 40 Index

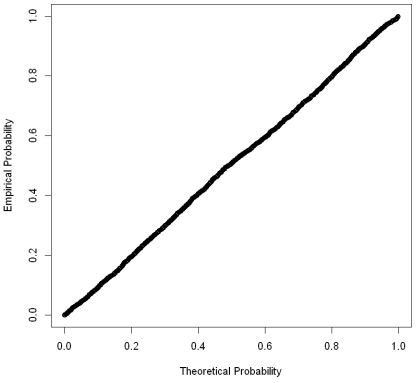

(b) JSE SWIX

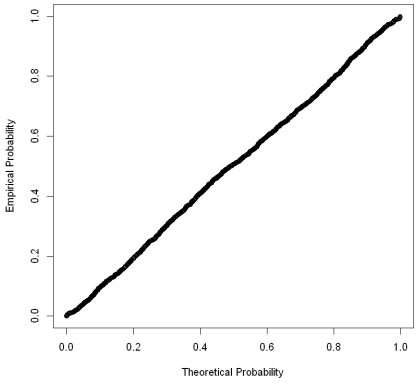

(c) JSE Financials Index

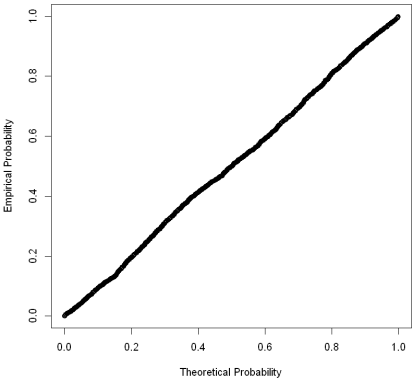

(d) JSE Resources Index

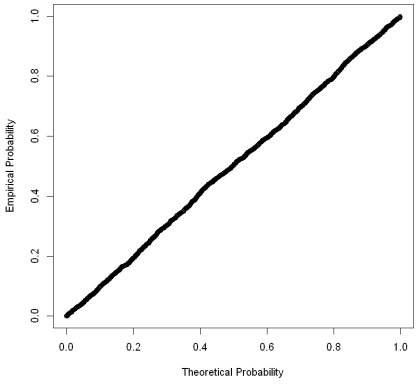

(e) JSE Industrials Index

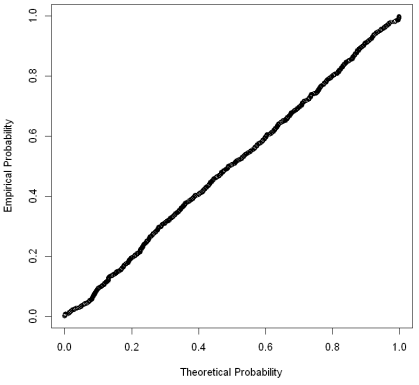

(f) JSE Banks Index

Figure 4.9: Variance Gamma P-P Plots

Table 4.5: Variance Gamma Distribution Parameter Estimates

	c	σ	θ	ν
JSE Top 40	0.002	0.011	-0.001	0.662
JSE SWIX	0.002	0.010	-0.002	0.666
JSE Financials	0.002	0.013	-0.001	0.774
JSE Resources	0.001	0.016	-0.001	0.675
JSE Industrials	0.003	0.011	-0.002	0.578
JSE Banks	0.002	0.0199	-0.002	0.852

Table 4.6: Kolmogorov-Smirnov Fit Statistics for the Variance Gamma Process

	D-Statistic	p-value
JSE Top 40	0.013	0.9849
JSE SWIX	0.013	0.9849
JSE Financials	0.015	0.9699
JSE Resources	0.018	0.8685
JSE Industrials	0.015	0.9614
JSE Banks	0.025	0.9733

4.1.3.1 Discussion

According to the KS test, there is no statistical evidence to reject the null hypothesis that the data is generated by the Variance Gamma process. The Q-Q plots, however, suggest that the Variance Gamma process underestimates probabilities in the tails of the data more than the Normal Inverse Gaussian process or the Generalized Hyperbolic process. Once again, care should be taken when using the Variance Gamma model for applications in which tail events are the primary concern.

4.1.4 Meixner Process

The theoretical densities of the Meixner process is overlain on the respective histograms below.

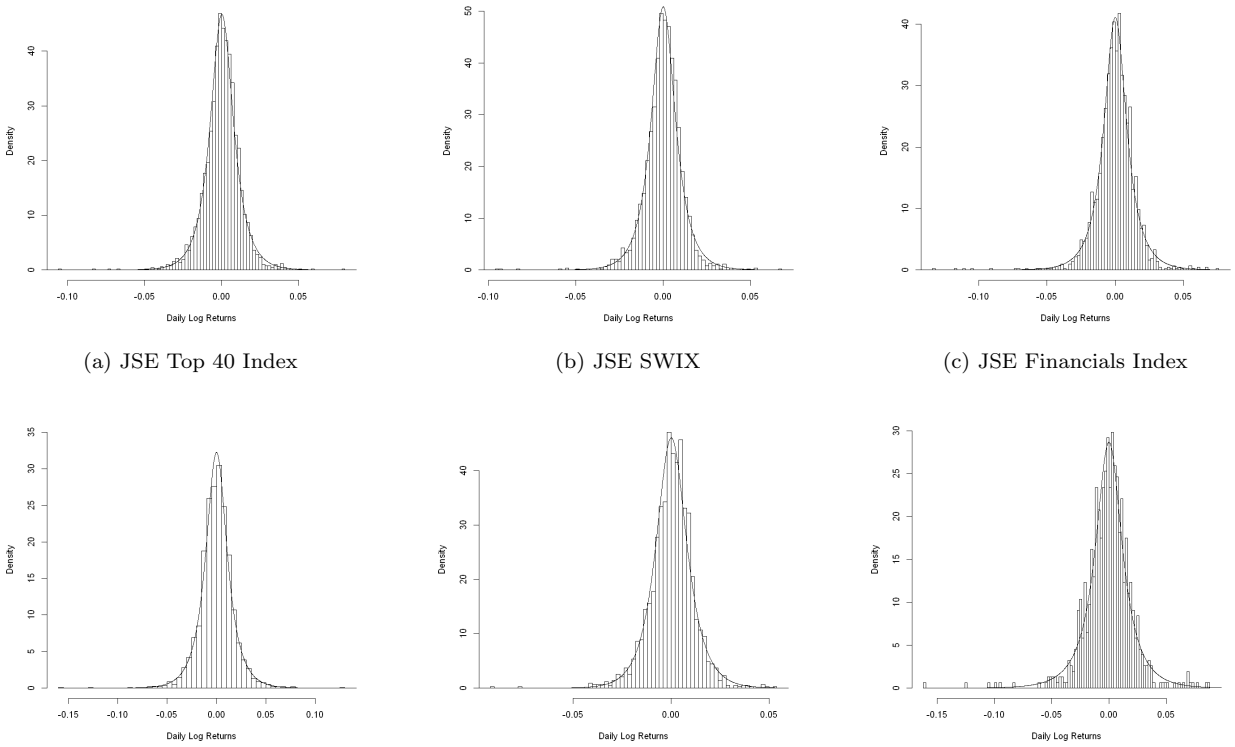

(a) JSE Top 40 Index (b) JSE SWIX (c) JSE Financials Index

(d) JSE Resources Index (e) JSE Industrials Index (f) JSE Banks Index

Figure 4.10: Meixner Density Plots

Q-Q Plots of the Meixner process are provided below.

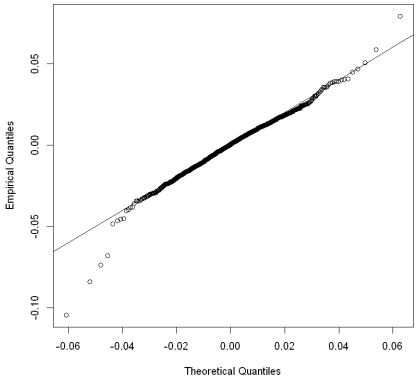

(a) JSE Top 40 Index

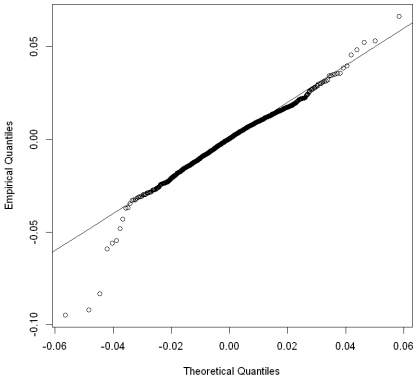

(b) JSE SWIX

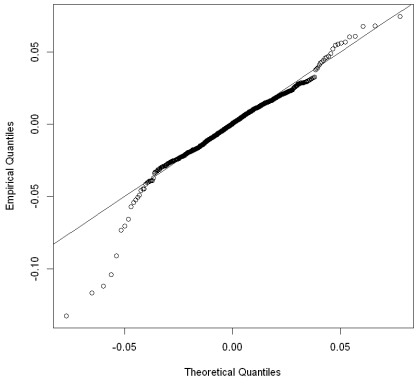

(c) JSE Financials Index

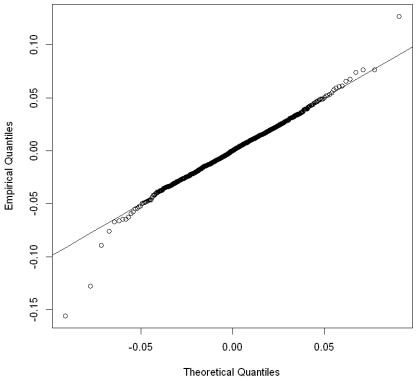

(d) JSE Resources Index

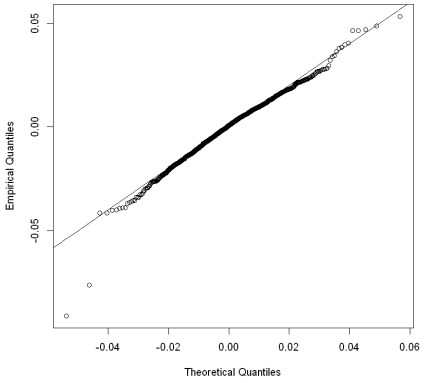

(e) JSE Industrials Index

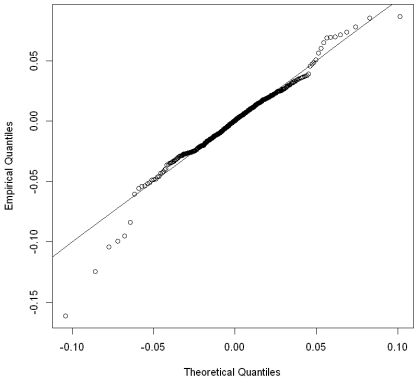

(f) JSE Banks Index

Figure 4.11: Meixner Q-Q Plots

P-P Plots of the Meixner process are provided below.

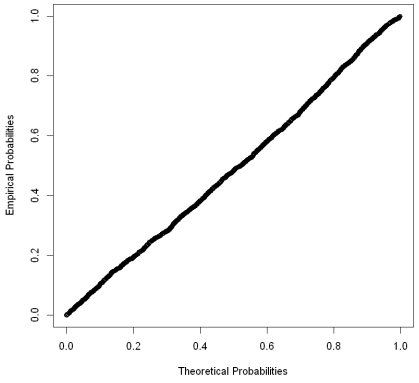

(a) JSE Top 40 Index

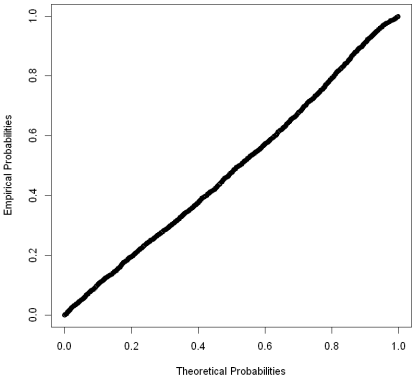

(b) JSE SWIX

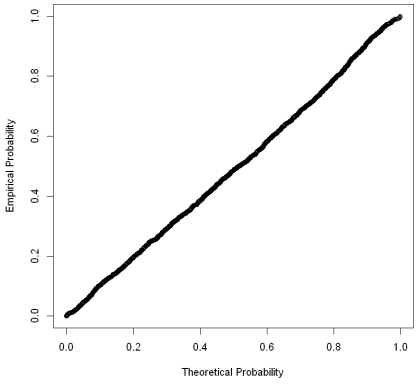

(c) JSE Financials Index

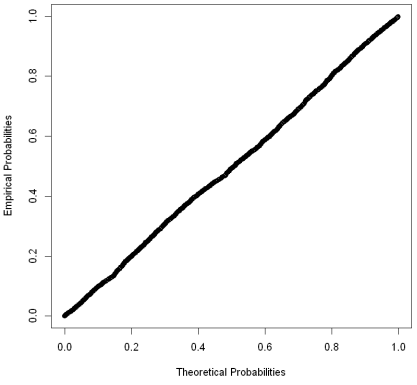

(d) JSE Resources Index

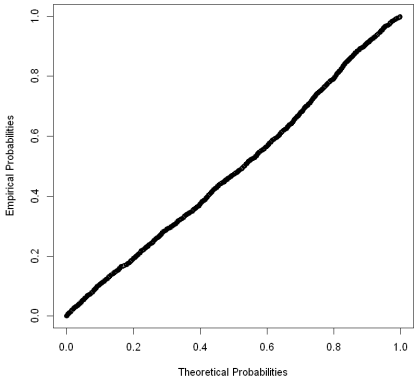

(e) JSE Industrials Index

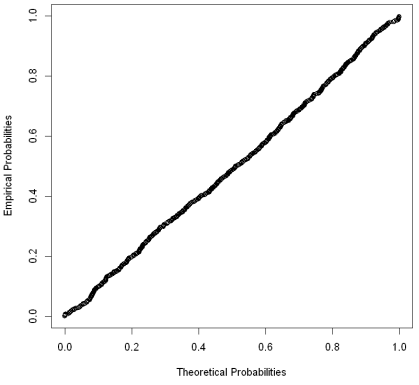

(f) JSE Banks Index

Figure 4.12: Meixner P-P Plots

Table 4.7: Meixner Distribution Parameter Estimates

	α	β	δ
JSE Top 40	0.026	0.048	0.387
JSE SWIX	0.024	0.050	0.377
JSE Financials	0.035	0.016	0.299
JSE Resources	0.040	-0.008	0.352
JSE Industrials	0.022	0.077	0.485
JSE Banks	0.057	-0.070	0.256

Table 4.8: Kolmogorov-Smirnov Fit Statistics for the Meixner Process

	D-Statistic	p-value
JSE Top 40	0.026	0.3362
JSE SWIX	0.032	0.1413
JSE Financials	0.026	0.4536
JSE Resources	0.016	0.9494
JSE Industrials	0.034	0.1555
JSE Banks	0.022	0.992

4.1.4.1 Discussion

The KS test statistics for the Meixner process are non-significant for all indices. According to the Q-Q plots and KS test, the Meixner process performs worse than the Normal Inverse Gaussian process, but uses fewer parameters and could thus be more stable with out of-sample-data. Further, the Meixner process seems to effectively capture the right tail of the data. Most financial applications concerned with tail events, however, consider the left tail. Thus, one should once again be careful when using the Meixner process for modeling tail events, since the Meixner process also underestimates the frequency of tail events.

4.2 QUANTUM MECHANICAL MODELS

4.2.1 Quantum Harmonic Oscillator

The theoretical densities of the Quantum Harmonic Oscillator is overlain on the respective histograms below.

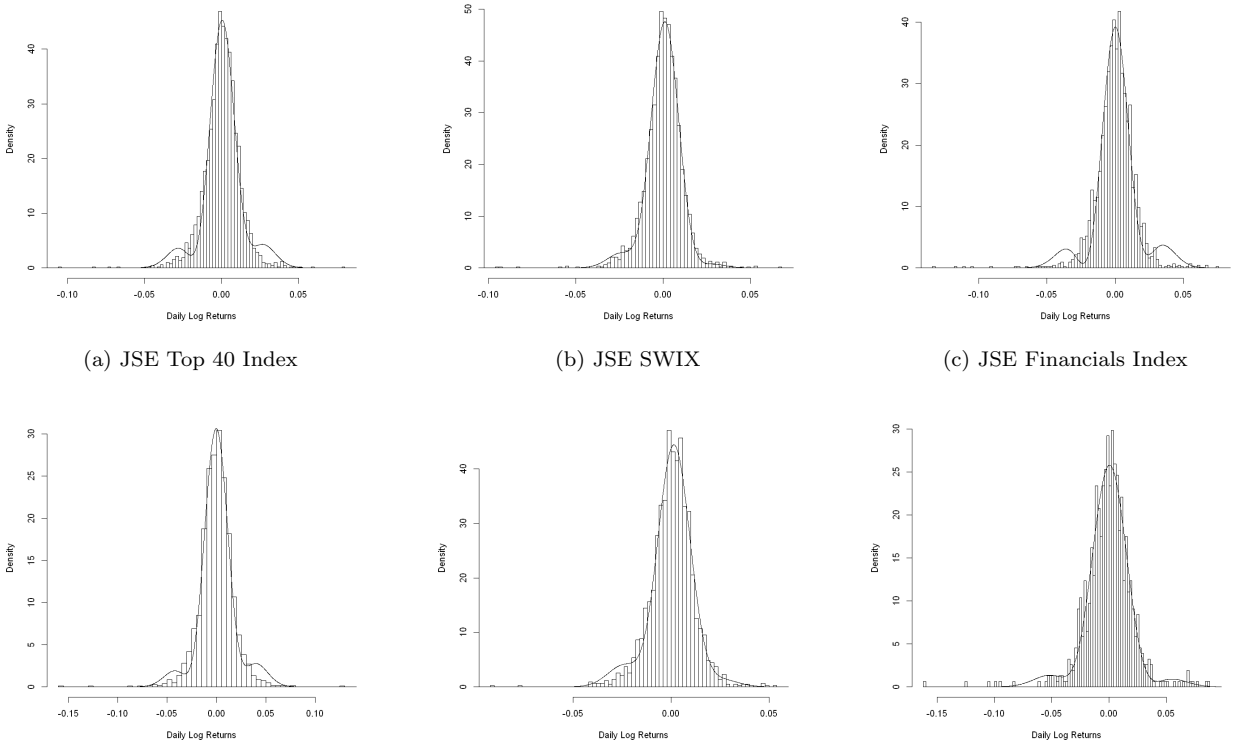

(a) JSE Top 40 Index (b) JSE SWIX (c) JSE Financials Index

(d) JSE Resources Index (e) JSE Industrials Index (f) JSE Banks Index

Figure 4.13: QHO Density Plots

Q-Q Plots of the Quantum Harmonic Oscillator are provided below.

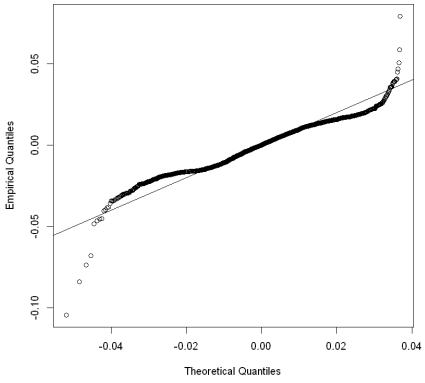

(a) JSE Top 40 Index

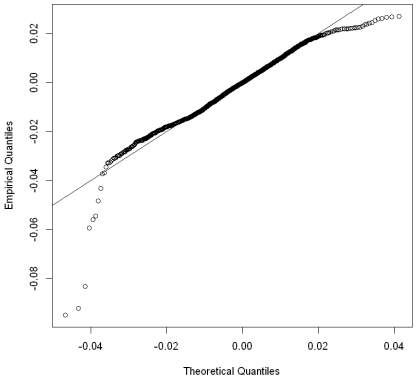

(b) JSE SWIX

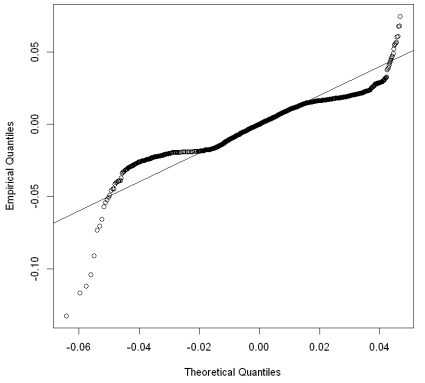

(c) JSE Financials Index

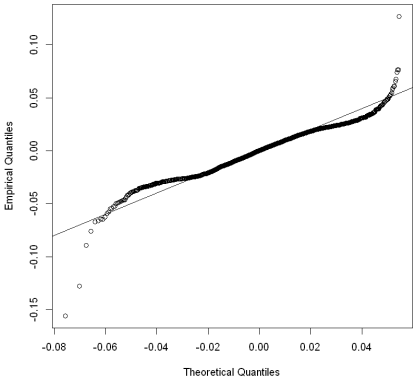

(d) JSE Resources Index

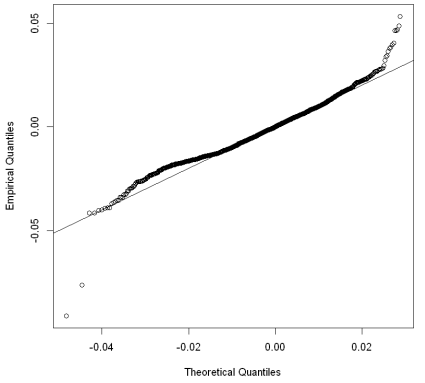

(e) JSE Industrials Index

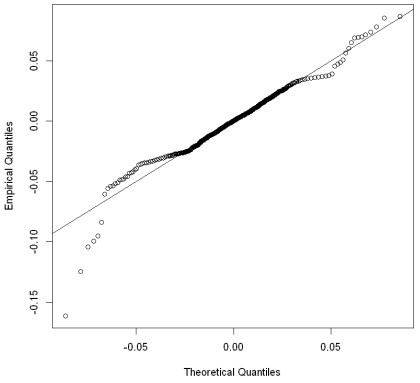

(f) JSE Banks Index

Figure 4.14: QHO QQ Plots

P-P Plots of the Quantum Harmonic Oscillator are provided below.

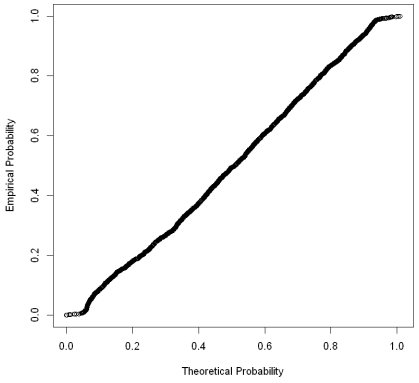

(a) JSE Top 40 Index

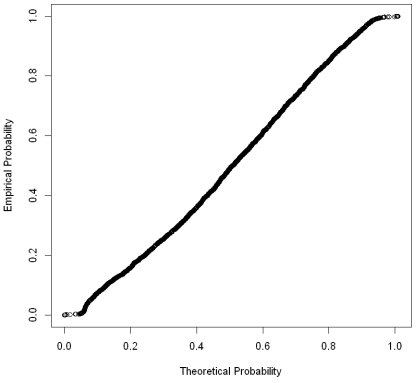

(b) JSE SWIX

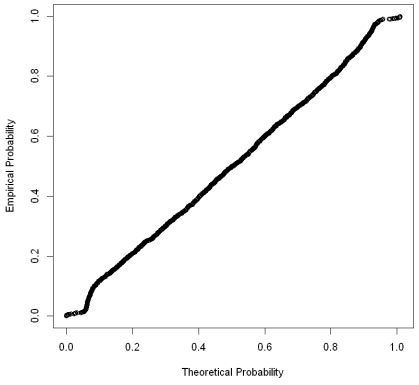

(c) JSE Financials Index

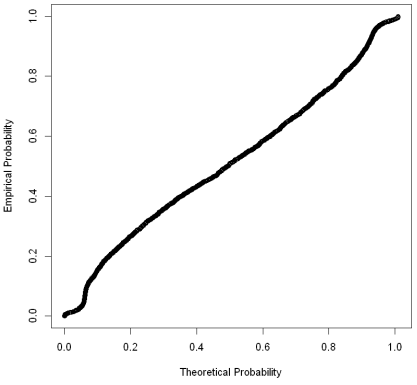

(d) JSE Resources Index

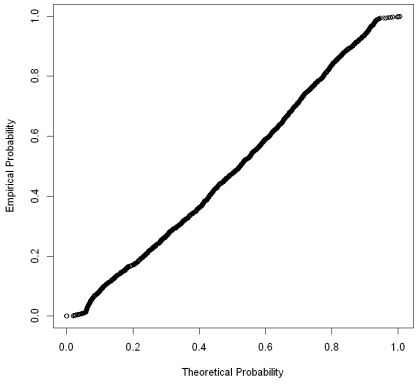

(e) JSE Industrials Index

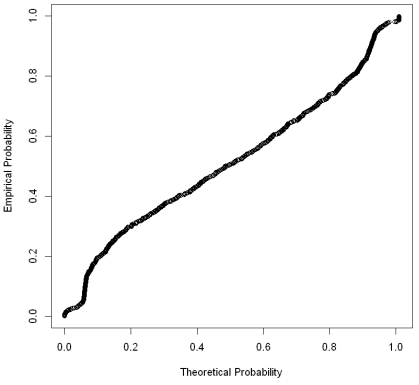

(f) JSE Banks Index

Figure 4.15: QHO PP Plots

Table 4.9: QHO Parameter Estimates

	$m\omega$	C_0	C_1	C_2	C_3	C_4
JSE Top 40	3.9909×10^{-31}	35.0546	1.725	2.7915	0.0062	1.3168
JSE SWIX	4.6079×10^{-31}	36.9211	-0.1438	-0.9473	-0.9436	0.7014
JSE Financials	2.6093×10^{-31}	28.3448	1.2631	2.3734	0.1178	1.3005
JSE Resources	1.8043×10^{-31}	23.5705	0.7605	1.3404	0.2728	0.8119
JSE Industrials	4.319×10^{-31}	36.467	0.4904	0.81264	-1.1478	0.7418
JSE Banks	1.1848×10^{-31}	18.91	-0.3417	-0.2634	-0.1736	0.5275

Table 4.10: Kolmogorov-Smirnov Fit Statistics for the QHO

	D-Statistic	p-value
JSE Top 40	0.051	0.002
JSE SWIX	0.058	0.0003
JSE Financials	0.04	0.062
JSE Resources	0.069	7.005×10^{-05}
JSE Industrials	0.053	0.005
JSE Banks	0.109	0.0002

4.2.1.1 Discussion

According to the KS test, at a significance level of 10%, the Quantum Harmonic Oscillator does not fit the data for any of the indices. The poor fit may be due to approximating the oscillator with only the first five eigenstates. Further analysis is needed to conclude with certainty that a Quantum Harmonic Oscillator, which includes more eigenstates, does not generate the daily log return process for the various indices. For practical purposes however, the computational expense of including more eigenstates makes the Quantum Harmonic Oscillator infeasible.

4.2.2 Quantum An-Harmonic Oscillator

The theoretical densities of the Generalized Hyperbolic process is overlain on the respective histograms below.

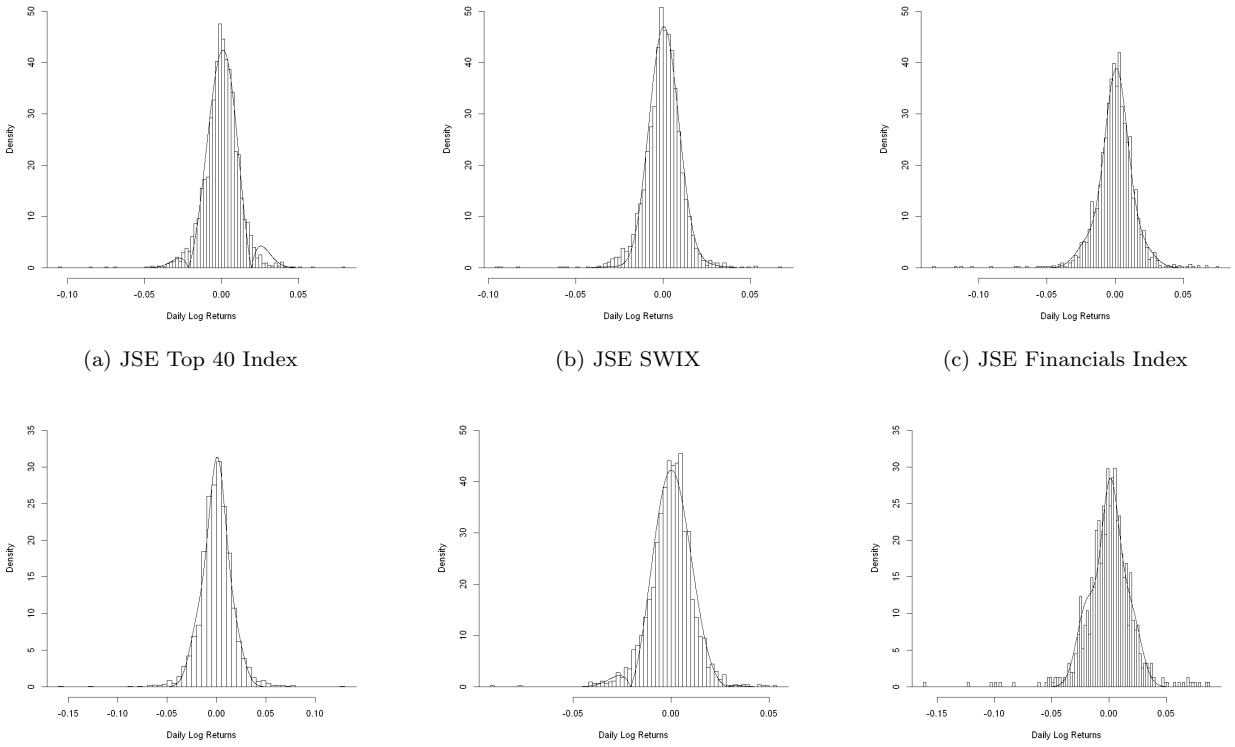

(a) JSE Top 40 Index (b) JSE SWIX (c) JSE Financials Index

(d) JSE Resources Index (e) JSE Industrials Index (f) JSE Banks Index

Figure 4.16: QAHO Density Plots

Q-Q Plots of the Quantum An-Harmonic Oscillator are provided below.

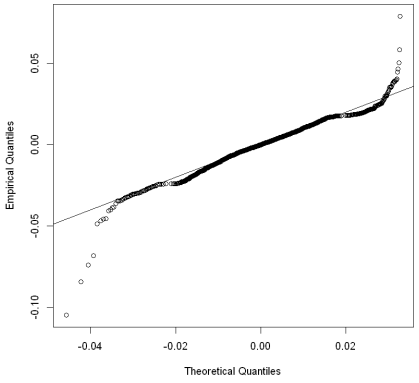

(a) JSE Top 40 Index

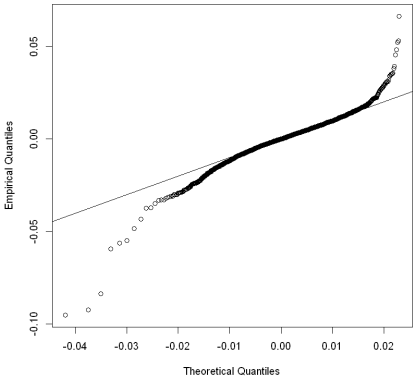

(b) JSE SWIX

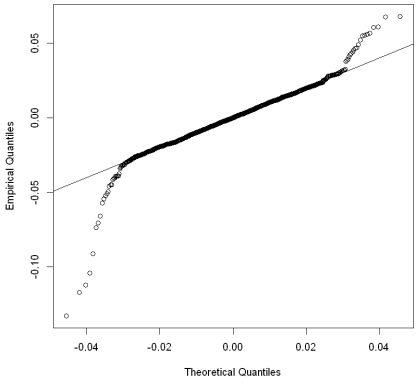

(c) JSE Financials Index

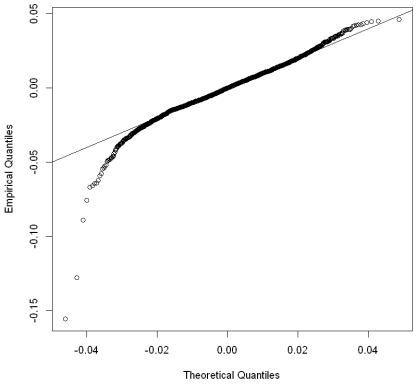

(d) JSE Resources Index

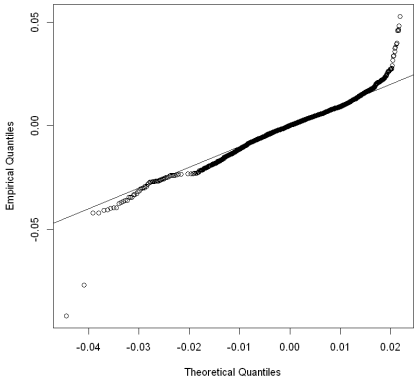

(e) JSE Industrials Index

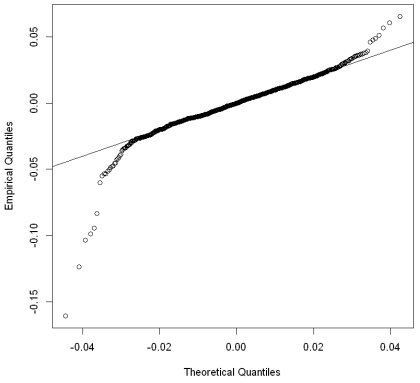

(f) JSE Banks Index

Figure 4.17: QAHO QQ Plots

P-P Plots of the Quantum An-Harmonic Oscillator are provided below.

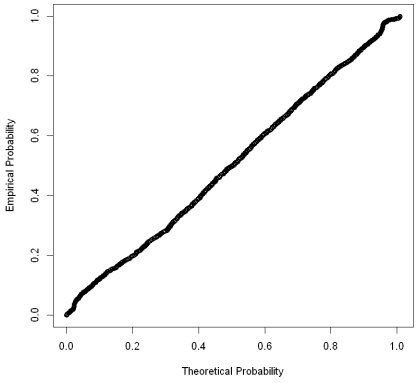

(a) JSE Top 40 Index

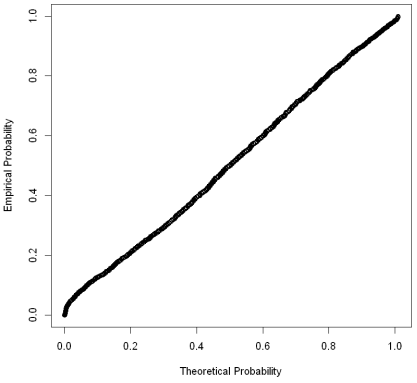

(b) JSE SWIX

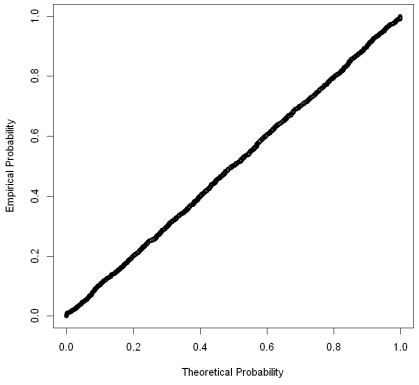

(c) JSE Financials Index

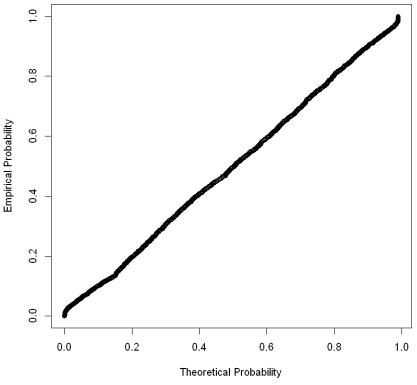

(d) JSE Resources Index

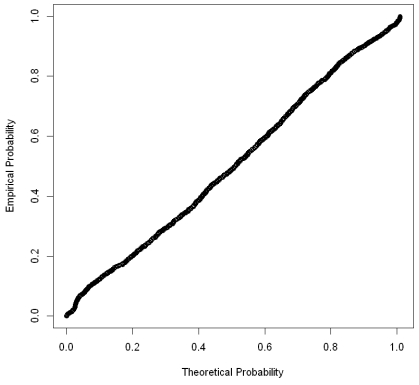

(e) JSE Industrials Index

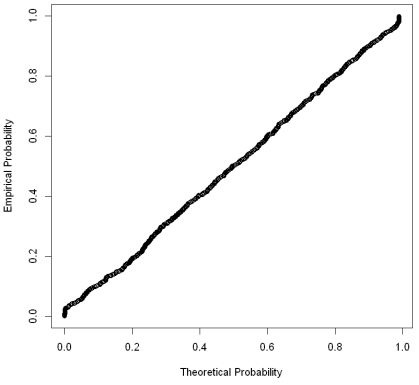

(f) JSE Banks Index

Figure 4.18: QAHO PP Plots

Table 4.11: QAHO Parameter Estimates

	m	α	β	C_0	C_1	C_2	C_3	C_4
JSE Top 40	9.1×10^{-18}	4.55×10^{-14}	9.1×10^{-15}	535.5134	−4.0103	−97.76686	−27.2728	−39.8529
JSE SWIX	9.1×10^{-18}	4.55×10^{-14}	9.1×10^{-15}	570.1517	−25.8396	−87.4033	−0.0689	19.8006
JSE Financials	9.1×10^{-18}	4.55×10^{-14}	9.1×10^{-15}	498.6316	−21.6085	−11.6037	−12.9782	40.2081
JSE Resources	9.1×10^{-18}	4.55×10^{-14}	9.1×10^{-15}	444.1511	−7.8036	57.3438	−10.7247	41.5994
JSE Industrials	9.1×10^{-18}	4.55×10^{-14}	9.1×10^{-15}	546.1558	−33.1762	−62.5891	22.3168	−17.8043
JSE Banks	9.1×10^{-18}	4.55×10^{-14}	9.1×10^{-15}	405.0857	−20.5871	86.9217	−17.1416	71.2443

Table 4.12: Kolmogorov-Smirnov Fit Statistics for the QAHO

	D-Statistic	p-value
JSE Top 40	0.027	0.3192
JSE SWIX	0.0343	0.0887
JSE Financials	0.009	1
JSE Resources	0.018	0.888
JSE Industrials	0.03	0.278
JSE Banks	0.025	0.973

4.2.2.1 Discussion

The KS test statistics for the Quantum An-Harmonic Oscillator are non-significant for all indices except the JSE SWIX, at a 10% significance level. The p-values are still low in comparison to the Lévy models, indicating that the Quantum An-Harmonic Oscillator does not fit the data as well as the Lévy models. Considering more eigenstates would likely improve the fit, but the computational expense and loss of accuracy due to discretization would make the Quantum An-Harmonic Oscillator impractical. Further, the Quantum An-Harmonic Oscillator severely underestimates the tails of the distribution according to the Q-Q plots.

CHAPTER 5

CONCLUSION

Chapter 1 provides evidence that daily log returns on financial indices are not generated by a Brownian Motion process. Chapter 2 and Chapter 3 then introduce alternative models in an attempt to find a model that accurately describes the distribution of log returns over the entire range of the data. Chapter 2 considers Lévy processes and Chapter 3 considers Quantum Mechanical models. The models described in Chapter 3 seem promising at face value, but do not hold up in the empirical study conducted in Chapter 4.

All of the Lévy processes analysed in Chapter 4 fit the log return data far better than the normal distribution. The Quantum Mechanical models perform poorly overall, and considering more complete approximations[1] would be impractical due to the computational expense. Overall, the Lévy models - particularly the Normal Inverse Gaussian model - are better choices for use in practice because they yield better goodness of fit results and are far less computationally expensive.

While the Lévy models give non-significant Kolmogorov-Smirnov test statistics, all of the models considered in this study perform poorly in the left tails of the distribution according to the Q-Q plots provided in Chapter 4. The Q-Q plots suggest that the tails of the theoretical distribution are thinner than the empirical distribution, and thus the probability of extreme events occurring will be underestimated. Therefore, in applications considering the tail of the distribution - such as Value at Risk - all of the models considered in this paper would most likely not be viable alternatives to Extreme Value Theory. The Lévy models would be the better choice amongst the models considered in applications concerned with the center of the distribution such as computing expected future values to price financial derivatives.

[1] More complete meaning to consider more eigenstates.

5.1 LIMITATIONS AND FURTHER RESEARCH

The interest of the study is in finding a distribution or family of distributions that performs well over the entire range of the log return data. This would allow the same model to be used for pricing derivatives and computing Value at Risk. The Kolmogorov-Smirnov test statistic considered has a weakness in that it is not sensitive to poor performance in the tails of the distribution. Better goodness of fit tests to consider would be the modified Kolmogorov-Smirnov test discussed in Mason and Schuenemeyer (1983) or the Anderson-Darling test discussed in Anderson (2011).

All models considered tend to underestimate the tails of the distribution, thus it may be beneficial to consider a mixture between the Normal Inverse Gaussian Distribution[2] and the General Pareto Distribution (GPD) commonly used in Extreme Value Theory.[3] The mixture would consist of a truncated Normal Inverse Gaussian Distribution over the region where the NIG performs well, and two GPD's (one for each tail) where the thresholds are equal to the truncation points. The GPD generally describes tail events well and the Normal Inverse Gaussian Distribution describes the center of the log return data accurately. Therefore, the mixture promises to provide an accurate fit over the entire range of the log return data.

[2]Recall that the NIG is the best performer of the models considered in the study.
[3]Refer to Beirlant *et al.* (2006) for a detailed discussion on the Generalized Pareto Distribution.

REFERENCES

Agarwal, R.P. and O'Regan, D. (2008). *Ordinary and partial differential equations: with special functions, Fourier series, and boundary value problems*. Springer Science & Business Media.

Ahn, K., Choi, M., Dai, B., Sohn, S. and Yang, B. (2018). Modeling stock return distributions with a quantum harmonic oscillator. *EPL (Europhysics Letters)*, vol. 120, no. 3, p. 38003.

Anderson, T.W. (2011). Anderson-darling tests of goodness-of-fit. *International Encyclopedia of Statistical Science*, vol. 1, pp. 52–54.

Ballotta, L. and Kyriakou, I. (2014). Monte carlo simulation of the cgmy process and option pricing. *Journal of Futures Markets*, vol. 34, no. 12, pp. 1095–1121.

Barndorff-Nielsen, O.E. (1997). Normal inverse gaussian distributions and stochastic volatility modelling. *Scandinavian Journal of Statistics*, vol. 24, no. 1, pp. 1–13.

Beirlant, J., Goegebeur, Y., Segers, J. and Teugels, J.L. (2006). *Statistics of extremes: theory and applications*. John Wiley & Sons.

Çinlar, E. (2011). *Probability and stochastics*, vol. 261. Springer Science & Business Media.

Cont, R. (2001). Empirical properties of asset returns: stylized facts and statistical issues. *Quantitative Finance*, vol. 1, pp. 223–236.

Drăgulescu, A.A. and Yakovenko, V.M. (2002). Probability distribution of returns in the heston model with stochastic volatility. *Quantitative finance*, vol. 2, no. 6, pp. 443–453.

Eberlein, E. and Hammerstein, E.A.v. (2004). Generalized hyperbolic and inverse gaussian distributions: limiting cases and approximation of processes. In: *Seminar on stochastic analysis, random fields and applications IV*, pp. 221–264. Springer.

Engle, R. (2004). Risk and volatility: Econometric models and financial practice. *American economic review*, vol. 94, no. 3, pp. 405–420.

Folks, J. and Chhikara, R. (1978). The inverse gaussian distribution and its statistical applications - a review. *Journal of the Royal Statistical Society.*, vol. 40, no. 3, pp. 1–13.

Gao, T. and Chen, Y. (2017). A quantum anharmonic oscillator model for the stock market. *Physica A: Statistical Mechanics and its Applications*, vol. 468, pp. 307–314.

Hull, J. (2009). *Options, futures and other derivatives*. Prentice Hall.

Konlack Socgnia, V. and Wilcox, D. (2014). A comparison of generalized hyperbolic distribution models for equity returns. *Journal of Applied Mathematics*, vol. 2014.

Lee, R.S. (2020). *Quantum Finance*. Springer.

LeVeque, R.J. (2007). *Finite difference methods for ordinary and partial differential equations: steady-state and time-dependent problems*. SIAM.

Madan, D.B., Carr, P.P. and Chang, E.C. (1998). The variance gamma process and option pricing. *Review of Finance*, vol. 2, no. 1, pp. 79–105.

Madan, D.B. and Seneta, E. (1990). The variance gamma (vg) model for share market returns. *Journal of business*, pp. 511–524.

Mason, D.M. and Schuenemeyer, J.H. (1983). A modified kolmogorov-smirnov test sensitive to tail alternatives. *The Annals of Statistics*, pp. 933–946.

Merton, R.C. (1976). Option pricing when underlying stock returns are discontinuous. *Journal of Financial Economics*, vol. 3, pp. 125–144.

Murphy, B. (1968). Handbook of methods of applied statistics. *Journal of the Royal Statistical Society: Series C (Applied Statistics)*, vol. 17, no. 3, pp. 293–294.

Petroni, N.C., De Martino, S. and De Siena, S. (1998). Exact solutions of fokker-planck equations associated to quantum wave functions. *Physics Letters A*, vol. 245, no. 1-2, pp. 1–10.

Pinsky, M. and Karlin, S. (2010). *An introduction to stochastic modeling*. Academic press.

Prause, K. (1999). *The generalized hyperbolic model: Estimation, financial derivatives and risk measures*. Ph.D. thesis.

Putz, M.V. (2019). *Quantum Nanochemistry, Volume Two: Quantum Atoms and Periodicity*. Apple Academic Press.

Rice, J.A. (2006). *Mathematical statistics and data analysis*. Cengage Learning.

Risken, H. and Frank, T. (1996). *Fokker-Planck Equation*. Springer.

Sakurai, J.J. and Commins, E.D. (1995). *Modern quantum mechanics, revised edition*. American Association of Physics Teachers.

Schoutens, W. (2002). *The Meixner process: Theory and applications in finance*. Eurandom Eindhoven.

Schoutens, W. (2003). *Lévy processes in finance: pricing financial derivatives*.

Shankar, R. (2012). *Principles of quantum mechanics*. Springer Science & Business Media.

Weisstein, E.W. (2020*a*). *Chi Distribution*.
Available at: `https://mathworld.wolfram.com/ChiDistribution.html`

Weisstein, E.W. (2020*b*). *Hermite Polynomial*.
Available at: `https://mathworld.wolfram.com/HermitePolynomial.html`

Wu, L. (2007). *Handbooks in operations research and management science*, vol. 15. Elsevier.

Zweibach, B. (2018). Chapter 1: Perturbation theory. *MIT Quantum Physics III Lecture Notes*.

APPENDIX A

BESSEL FUNCTIONS

This appendix serves to introduce the reader to the basic ideas behind Bessel functions. For a more in depth discussion on the topic, the reader is referred to Agarwal and O'Regan (2008).

Bessel functions are solutions to Bessel's differential equation:

$$x^2y''(x) + xy'(x) + \left(x^2 - a^2\right)y(x) = 0 \tag{A.1}$$

It can be shown that a power series solution to (A.1) can be obtained as:

$$y(x) = x^r \sum_{m=0}^{\infty} c_m x^m \tag{A.2}$$

Substituting (A.2) into (A.1) gives:

$$c_0(r+a)(r-a) = 0 \tag{A.3a}$$

$$c_1(1+r+a)(1+r-a) = 0 \tag{A.3b}$$

$$c_m(m+r+a)(m+r-a) = -c_{m-2},\ m = 2, 3, ... \tag{A.3c}$$

Assuming $c_0 \neq 0$, the solution to (A.3) is $r_1 = a$ and $r_2 = -a$.

Now, in the case where $r_1 - r_2 = 2a$ is not an integer, the solutions to (A.1) are:

$$y_1(x) = \sum_{x=0}^{\infty} \frac{(-1)^m}{m!\Gamma(m+1-a)} \left(\frac{x}{2}\right)^{2m-a} \tag{A.4a}$$

and

$$y_2(x) = \sum_{x=0}^{\infty} \frac{(-1)^m}{m!\Gamma(m+1+a)} \left(\frac{x}{2}\right)^{2m+a} \tag{A.4b}$$

Equation (A.4a) is called the Bessel function of the first kind of order a. Equation (A.4b) is called

the Bessel function of the first kind of order $-a$. A Bessel function of the first kind and of order a is denoted $J_a(x)$. Solutions to the case where $r_1 - r_2$ is an odd integer is an extension of the solution obtained in (A.4), and the reader is encouraged to refer to Agarwal and O'Regan (2008).

In the event that $r_1 - r_2 = a$ is an even integer, $y_1(x) = J_a(x)$ again. However, the solution to $y_2(x)$ is obtained as:

$$\begin{aligned} y_2(x) =& \frac{2}{\pi}\left[\left(\gamma + \ln\left|\frac{x}{2}\right|\right) J_a(x) - \frac{1}{2}\sum_{m=0}^{a-1}\frac{(a-1-k)!}{k!}\left(\frac{x}{2}\right)^{2k-a}\right] \\ &+ \frac{2}{\pi}\left[\frac{1}{2}\sum_{m=0}^{\infty}(-1)^{m+1}\frac{\phi(m)+\phi(a+m)}{m!(a+m)!}\left(\frac{x}{2}\right)^{2m+a}\right] \end{aligned} \tag{A.5}$$

with $\phi(0) = 0,\ \phi(m) = \sum_{k=1}^{m}\left(\frac{1}{k}\right)$ and γ the Euler constant:

$$\gamma = \lim_{m\to\infty}\left(\phi(m) - \ln m\right) \approx 0.5772157$$

The solution of $y_2(x)$ in (A.5) is referred to as Weber's Bessel function of the second kind,[1] and is denoted $Y_a(x)$.

Bessel functions of the third kind[2] are the complex solutions to (A.1), defined by:

$$H_a^{(1)}(x) = J_a(x) + iY_a(x) \tag{A.6a}$$

and

$$H_a^{(2)}(x) = J_a(x) + iY_a(x) \tag{A.6b}$$

Modified Bessel functions are solutions to the modified Bessel differential equation:

$$x^2y''(x) + xy'(x) - \left(x^2 + n^2\right)y(x) = 0 \tag{A.7}$$

[1] Weber's Bessel function is sometimes referred to as the Neumann function.
[2] Bessel functions of the third kind are sometimes called Hankel functions.

A modified Bessel function of the first kind and of order a is:

$$I_a(x) = i^{-a} J_a(ix) = e^{-\frac{a\pi i}{2}} J_a(ix) \tag{A.8}$$

The modified Bessel function of the second kind and of order a is:

$$K_a(x) = \begin{cases} \dfrac{\pi}{2}\left[\dfrac{I_{-a}(x) - I_a(x)}{\sin(a\pi)}\right], & a \neq 0, 1, 2, 3, ... \\ \lim\limits_{p \to a} \dfrac{\pi}{2}\left[\dfrac{I_{-p}(x) - I_a(x)}{\sin p\pi}\right], & a = 0, 1, 2, 3, ... \end{cases} \tag{A.9}$$

APPENDIX B

OVERVIEW OF DIRAC NOTATION

The bra-ket notation introduced by Dirac makes it easier to represent certain abstract mathematical objects used in Quantum Mechanics. This appendix defines the notation and provides an overview of the linear algebra used in Chapter 3. For a more detailed discussion, see Shankar (2012).

B.1 NOTATION AND DEFINITIONS

- $|\psi\rangle$ is analogous to a column vector and is referred to in the literature as a ket vector.
- The conjugate transpose of $|\psi\rangle$ - denoted $|\psi\rangle^\dagger$ - is $\langle\psi|$. This is analogous to a row vector in linear algebra and is called the bra vector.
- An operator[1] is analogous to a square matrix in linear algebra.
- $\langle\psi|\phi\rangle$ is an inner product between $\langle\psi|$ and $|\phi\rangle$.
- An operator is called Hermitian if $H^\dagger = H$.

B.2 FUNCTIONS AS VECTORS

A function can be thought of as a vector in the following manner: Consider a function, say $f(x)$, with discrete domain. Then $f(x)$ can be represented by the inner product $\langle x|f\rangle$, where x is a vector of size n containing $n-1$ zeros and a one at the point of interest. f is a vector that contains the values of f in an order corresponding to its domain. A function can then be thought of as a continuous extension of this idea.

[1] Such as the Hamiltonian operator.

APPENDIX C

PERTURBATION THEORY FOR SOLVING THE QFSE

This appendix briefly describes the perturbation theory required to obtain approximate solutions to the Quantum An-Harmonic Oscillator. The discussion presented is based on Zweibach (2018). Only the non-degenerate cases are considered in this overview.[1]

Recall the Hamiltonian of the QFSE:[2]

$$\hat{H}_{\text{QFSE}} = -\frac{\hbar}{2m}\frac{d^2}{dr^2} + \frac{\gamma^*\eta\delta}{2}r^2 + \frac{\gamma^*\eta\nu}{4}r^4$$

Now, let $\frac{\gamma^*\eta\delta}{2} = \frac{m\omega^2x^2}{2}$ so that $\hat{H}_{\text{QFSE}}$ can be written as:

$$\hat{H}_{\text{QFSE}} = \hat{H}^{(0)} + \delta\hat{H}$$

Where $\hat{H}^{(0)} = -\frac{\hbar}{2m}\frac{d^2}{dr^2} + \frac{m\omega^2x^2}{2}$ is the well know Hamiltonian of the Quantum Harmonic Oscillator for which algebraic forms of the eigenstates and eigeneregies are well known.

The next step is to introduce a parameter $\lambda\ \epsilon\ [0, 1]$, so that for a general Hamiltonian:

$$\hat{H}(\lambda) = \hat{H}^{(0)} + \lambda\delta\hat{H}$$

Where $\hat{H}(\lambda)$, $\hat{H}^{(0)}$ and $\hat{H}$ are all Hermitian. The Hamiltonian is now expresses as a well known Hamiltonian[3] plus some perturbation. When $\lambda = 0$ the well known case is obtained, and when $\lambda = 1$ the Hamiltonian to be solved is obtained.

[1] Non-degenerate cases are cases where the well known Hamiltonian has non-repeating eigenenergies and eigenstates.

[2] Equation 3.54.

[3] Not necessarily that of the Harmonic Oscillator.

First, assume that $\hat{H}^{(0)}$ has discrete allowed energy levels and an an orthonormal basis $|k^{(0)}\rangle$ of energy eigenstates. $k^{(0)} \epsilon \{0, 1, 2, 3, 4, ...\}$ is a label for the various allowed energy eigenstates of a system with Hamiltonian $\hat{H}^{(0)}$:

$$\hat{H}^{(0)} |k^{(0)}\rangle = E_k^{(0)} |k^{(0)}\rangle, \qquad \langle k^{(0)}|l^{(0)}\rangle = \delta_{kl}$$

In general $k = 0$ is the ground state, and the eigeneregies are ordered to be increasing. Now, as λ increases from 0 to 1, the energy eigenstate $|k^{(0)}\rangle$ of $\hat{H}^{(0)}$ will evolve into an energy eigenstate $|k\rangle_\lambda$ of $\hat{H}(\lambda)$ and:

$$\hat{H}(\lambda) |k\rangle_\lambda = E_n(\lambda) |k\rangle_\lambda$$

Analogous to taking a Taylor Series Expansion, consider:

$$|k\rangle_\lambda = |k^{(0)}\rangle + \lambda |k^{(1)}\rangle + \lambda^2 |k^{(2)}\rangle + ... \tag{C.1}$$

$$E_k(\lambda) = E_k^{(0)} + \lambda E_k^{(1)} + \lambda^2 E_k^{(2)} + ... \tag{C.2}$$

i.e. the perturbed state is the well known state plus some correction.

The Schrödinger Equation can now be rewritten as:

$$\left(\hat{H}^{(0)} + \lambda \delta \hat{H} - E_k(\lambda)\right) |k\rangle_\lambda = 0$$

Using (C.1) and (C.2):

$$\left(\left(\hat{H}^{(0)} - E_k^{(0)}\right) - \lambda \left(E_k^{(1)} - \delta \hat{H}\right) - \lambda^2 E_k^{(2)} - \lambda^3 E_k^{(3)} - ... - \lambda^n E_k^{(n)} + ...\right)$$

$$\left(|k^{(0)}\rangle + \lambda |k^{(1)}\rangle + \lambda^2 |k^{(2)}\rangle + \lambda^3 |k^{(3)}\rangle + ... + \lambda^n |k^{(n)}\rangle + ...\right) = 0$$

Collect the coefficients of λ:

$$
\begin{aligned}
\lambda^0: &\quad \left(\hat{H}^{(0)} - E_k^{(0)}\right)|k^{(0)}\rangle = 0 \\
\lambda^1: &\quad \left(\hat{H}^{(0)} - E_k^{(0)}\right)|k^{(1)}\rangle = \left(E_k^{(1)} - \delta\hat{H}\right)|k^{(0)}\rangle \\
\lambda^2: &\quad \left(\hat{H}^{(0)} - E_k^{(0)}\right)|k^{(2)}\rangle = \left(E_k^{(1)} - \delta\hat{H}\right)|k^{(1)}\rangle + E_k^{(2)}|k^{(0)}\rangle \\
&\vdots \\
\lambda^n: &\quad \left(\hat{H}^{(0)} - E_k^{(0)}\right)|k^{(n)}\rangle = \left(E_k^{(1)} - \delta\hat{H}\right)|k^{(n-1)}\rangle + E_k^{(2)}|k^{(n-2)}\rangle + ... + E_k^{(n)}|k^{(0)}\rangle
\end{aligned}
$$

Zweibach (2018) then goes on to show that the $|k^{(n)}\rangle$'s can be chosen to be orthonormal.

Left multiplying the λ^1 equation by $\langle k^{(0)}|$ gives:

$$
\begin{aligned}
0 &= E_k^{(1)}\langle k^{(0)}|k^{(0)}\rangle - \delta\langle k^{(0)}|\hat{H}|k^{(0)}\rangle \\
\Rightarrow E_k^{(1)} &= \langle k^{(0)}|\delta\hat{H}|k^{(0)}\rangle
\end{aligned}
$$

and it can be shown that in general that:

$$
E_k^{(n)} = \langle k^{(0)}|\delta\hat{H}|k^{(n-1)}\rangle
$$

Now the state correction must be found. For the first state correction - $|k^{(1)}\rangle$:

$$
\left(\hat{H}^{(0)} - E_k^{(0)}\right)|k^{(1)}\rangle = \left(E_k^{(1)} - \delta\hat{H}\right)|k^{(0)}\rangle
$$

Left multiplying by $\langle l^{(0)}|$, $l \neq k$:

$$
\langle l^{(0)}|\left(\hat{H}^{(0)} - E_k^{(0)}\right)|k^{(1)}\rangle = \langle l^{(0)}|\left(E_k^{(1)} - \delta\hat{H}\right)|k^{(0)}\rangle
$$

To simplify the notation, let $\delta H_{mn} = \langle m^{(0)}|\delta\hat{H}|n^{(0)}\rangle$. Note that due to $\hat{H}$ being Hermitian, $\delta H_{nm} = (\delta H_{mn})^*$.[4]

[4] X^* represents the conjugate transpose of X.

Now:

$$\langle l^{(0)}|k^{(1)}\rangle = -\frac{\delta H_{lk}}{E_l^{(0)} - E_k^{(0)}}, \qquad l \neq k$$

It is well known that $\sum_k |k^{(0)}\rangle \langle k^{(0)}| = 1$, because the $k^{(0)}$'s are orthonormal. So the above equation is left multiplied by $\sum_l |l^{(0)}\rangle$, and the first order state correction is obtained:

$$|k^{(1)}\rangle = -\sum_{l\neq k} \frac{|l^{(0)}\rangle\, \delta H_{lk}}{E_l^{(0)} - E_k^{(0)}}$$

To compute the correction is difficult because all other states must be known,[5] and is out of the scope of this project.[6]

[5] Which for the QHO is an infinite amount.
[6] Some background is required and the reader is referred to Zweibach (2018).